QED positivity bounds

Lasma Alberte,[1,*] Claudia de Rham,[1,2,†] Sumer Jaitly,[1,‡] and Andrew J. Tolley[1,2,§]

[1]*Theoretical Physics, Blackett Laboratory, Imperial College, London SW7 2AZ, United Kingdom*
[2]*CERCA, Department of Physics, Case Western Reserve University, 10900 Euclid Avenue, Cleveland, Ohio 44106, USA*

(Received 29 January 2021; accepted 24 May 2021; published 22 June 2021)

We apply positivity bounds directly to a $U(1)$ gauge theory with charged scalars and charged fermions, i.e., QED, minimally coupled to gravity. Assuming that the massless t-channel pole may be discarded, we show that the improved positivity bounds are violated unless new physics is introduced at the parametrically low scale $\Lambda_{\rm new} \sim (emM_{\rm Pl})^{1/2}$, consistent with similar results for scalar field theories, far lower than the scale implied by the weak gravity conjecture. This is sharply contrasted with previous treatments which focus on the application of positivity bounds to the low energy gravitational Euler-Heisenberg effective theory only. We emphasize that the low cutoff is a consequence of applying the positivity bounds under the assumption that the pole may be discarded. We conjecture an alternative resolution that a small amount of negativity, consistent with decoupling limits, is allowed and is not in conflict with standard UV completions, including weakly coupled ones.

DOI: 10.1103/PhysRevD.103.125020

I. INTRODUCTION

It is now well established that for nongravitational quantum field theories to admit a local Lorentz invariant unitary UV completion, the low energy scattering amplitude should satisfy an array of positivity bounds that constrain the sign and magnitude of Wilson coefficients. The simplest bounds were first noted in [1–3], and the connection between their violation and causality was emphasized in [3]. These original forward limit scalar bounds have been extended to general spins [4,5] away from the forward limit [5,6]. These bounds have proven fruitful in placing constraints on interacting spin-2 fields [7–14], restricting beyond standard model interactions [15–24], and providing a new light on properties of string amplitudes [25,26]. Most recently it has been recognized that by using more information from crossing symmetry and the partial wave expansion it is possible to put upper and lower bounds on Wilson coefficients [27–31] in certain cases ruling out classes of theories from having a standard UV completion such as weakly broken Galileon theories [27,28]. Similar results are arrived at within the related S-matrix bootstrap program [32].

Given these successes, it is highly desirable to consider the impact of these bounds for realistic effective field theories coupled to gravity. Unfortunately, the direct application of positivity bounds to gravitational effective field theories is fraught with difficulties. On the one hand, the distinctive features of gravity mean that scattering amplitudes are permeated by massless poles and branch points which spoil the conventional forward limit considerations, and preclude an analytic continuation from the physical region which preserves positivity even away from the forward limit. On the other hand, causality in the gravitational setting is more subtle, from the ambiguity of the metric under field redefinitions and known superluminal speeds in well established low energy effective field theories (EFTs) [33–36]. In a previous paper [37], we argued that the only gravitational effective theories in which positivity is clear-cut are those for which there is a clean $M_{\rm Pl} \to \infty$ decoupling limit, for which positivity of the nongravitational decoupling limit theory may be assured. With this in mind, we considered several examples of renormalizable scalar field theories coupled to gravity for which violations of positivity are necessarily suppressed by powers of $M_{\rm Pl}$. Demanding the scattering amplitude respects positivity with the gravitational t-channel pole removed generically imposes the cutoff of the effective theory to be far lower than expected, a result which parallels conclusions from the swampland program [38,39].

In the present work we extend the results of [37] to the more interesting case of QED minimally coupled to gravity.

*l.alberte@imperial.ac.uk
†c.de-rham@imperial.ac.uk
‡sumer.jaitly14@imperial.ac.uk
§a.tolley@imperial.ac.uk

Unlike in Ref. [37], we will not rely on the device of introducing a spectator field, but rather consider the improved positivity bounds [4,9,10]. In their simplest form, the standard forward limit positivity bounds can be applied on the pole-subtracted scattering amplitudes as [3]

$$\frac{\mathrm{d}^2\mathcal{A}_i(s,0)}{\mathrm{d}s^2} = \frac{2}{\pi}\int_{4m^2}^{\infty}\mathrm{d}\mu\,\frac{\mathrm{Im}\mathcal{A}_i(\mu,0)}{(\mu-s)^3} + \frac{2}{\pi}\int_{4m^2}^{\infty}\mathrm{d}\mu\,\frac{\mathrm{Im}\mathcal{A}_i^c(\mu,0)}{(\mu-u)^3} > 0, \quad (1.1)$$

where the positivity of the expression (for $0 < s < 4m^2$, $u = 4m^2 - s$) on the left-hand side arises due to the analyticity properties of the S-matrix and positivity from the optical theorem, and A_i^c is the $s-u$ crossing exchanged amplitude. The improved positivity bounds [4,9,10] allow us to tighten the bound by including any additional knowledge about our EFT. The idea behind them is particularly transparent from the exact formulation of the optical theorem as

$$\mathrm{Im}\mathcal{A}_i(s,0) = \frac{1}{2}\sum_f\int\mathrm{d}\Pi_f|\mathcal{A}_{i\to f}|^2 > 0, \quad (1.2)$$

where i denotes the initial and final particle content, f stands for any intermediate state, and $\mathrm{d}\Pi_f$ is the phase space volume. The theorem then implies that, given a set of possible intermediate states in the theory that is being investigated, i.e., $\{f_1, f_2, \ldots, f_N\}$, each known contribution to the sum on the right-hand side of the above equation can be taken to the left-hand side leading to an even tighter constraint on the remaining amplitudes. This gives the improved positivity bounds

$$\frac{\mathrm{d}^2\mathcal{A}_i(s,0)}{\mathrm{d}s^2} - \frac{1}{\pi}\sum_{\mathrm{known}f}\int\mathrm{d}\Pi_f\int_{4m^2}^{\infty}\mathrm{d}\mu\,\frac{|\mathcal{A}_{i\to f}|^2}{(\mu-s)^3} - \frac{1}{\pi}\sum_{\mathrm{known}f}\int\mathrm{d}\Pi_f\int_{4m^2}^{\infty}\mathrm{d}\mu\,\frac{|\mathcal{A}_{i\to f}^c|^2}{(\mu-u)^3} > 0, \quad (1.3)$$

where overall positivity is still ensured by the sum over "unknown" configurations f. It is in the application of improved positivity bounds that our results will differ from previous discussions of positivity bound for QED coupled to gravity, notably [40], and more recently [41–43] which have focused entirely on the gravitational Euler-Heisenberg effective field theory that describes physics well below the electron mass.[1] The latter is sufficient to reproduce the bounds (1.1), but by preserving information from physics at and above the electron mass, one is able to derive a much tighter constraint as implied by the improved bound (1.3).

Remarkably, the authors of [40] noted that if positivity bounds were applied to four-photon (i.e., 2-2) scattering amplitudes with the gravitational t-channel exchange removed,[2] positivity would hold if the general requirements of the weak gravity conjecture [54] are met, namely that there is a bound on the charge to mass ratio $|e|/m \gtrsim 1/M_{\mathrm{Pl}}$. Interestingly, at least in three dimensions (3D), this observation is partly countered by that of [43] which uses the extended positivity bounds of [31] to derive opposing bounds, arguing for the need for additional light neutral states to resolve this tension. As we discuss in Sec. IV D, this particular "resolution" does not apply in the four-dimensional case considered here.

Keeping in the spirit of applying positivity bounds to the t-channel removed amplitude, we shall find a much stronger result: *Improved positivity bounds applied to QED coupled to gravity demand the existence of new physics at the scale* $\Lambda_{\mathrm{new}} \sim (emM_{\mathrm{Pl}})^{1/2}$. Most importantly this result is independent of what that new physics is. For instance, it applies equally well for the Regge-like completions considered in [41] where the photon Regge tower dominates over the graviton tower, and it is argued that the weak gravity conjecture from a positivity argument is robust. That is because any Lorentz invariant UV completion will be described at low energies as irrelevant operators correcting the naive QED Lagrangian, and our consideration only demands that some new physics comes in at the scale $\Lambda_{\mathrm{new}} \sim (emM_{\mathrm{Pl}})^{1/2}$, which would show up at low energies as the need to add irrelevant operators, but makes no demands to what its origin is.

As discussed in [37] an alternative explanation of our results is that strict positivity of the scattering amplitude, with the t-channel pole removed, does not apply. Indeed, we can only be sure it applies in the decoupling limit $M_{\mathrm{Pl}} \to \infty$. Rather in [37] we conjectured that in the gravitational context, for a scattering amplitude whose low energy expansion near $t = 0$ takes the form[3]

$$\mathcal{A} \sim -\frac{s^2}{M_{\mathrm{Pl}}^2 t} + cs^2 + \cdots, \quad (1.4)$$

[1]This information is partly recovered in the 3D case considered in [43] by focusing on the large order limit in an expansion in s/m^2. In practice, for our considerations it is better to utilize the improved positivity bounds since the former is dominated by the branch put at $4m^2$ and the latter at a much higher scale.

[2]These bounds can be motivated on entropic grounds [44–47] or in other setups [48–51]. Recently, the procedure of applying directly the positivity bounds to the t-channel removed amplitude was argued to be justified by a compactification argument in [42]. In [37] various issues with this compactification argument were pointed out. See also [52,53] for related discussions.

[3]In general graviton loops lead to branch cuts extending to $t = 0$; however, for the four-photon amplitude these necessarily arise at order $1/M_{\mathrm{Pl}}^4$ and so will not affect any considerations here. Nevertheless, they are indicative of the issues with continuing the partial wave expansion past $t = 0$.

the standard positivity bound (1.1) is weakened to the requirement

$$c > -\frac{\mathcal{O}(1)}{M^2 M_{\rm Pl}^2}, \tag{1.5}$$

where M is at most the cutoff Λ_c of the low energy expansion $M \leq \Lambda_c$. This weakening is consistent with the known weakening of causality criteria in familiar EFTs [33–36]. Our results for QED indicate that the improved positivity bound (1.3) would need to be weakened to

$$c^{\rm imp} > -\frac{e^2}{m^2 M_{\rm Pl}^2} \times \mathcal{O}(1), \tag{1.6}$$

where m is the electron mass to avoid the need to introduce new physics at the scale $\Lambda_{\rm new} \sim (emM_{\rm Pl})^{1/2}$. Here $c^{\rm imp}$ is the equivalent coefficient that arises in the expansion of the improved amplitude (3.8). This is consistent with (1.5) for $M \sim m/e$. While (1.6) is not in conflict with the $M_{\rm Pl} \to \infty$ decoupling limit, it would nevertheless indicate a significant weakening of positivity that deserves further explanation. At present there is no generally accepted proof of positivity of c at finite $M_{\rm Pl}$.

We stress again that our conclusions are valid for generic standard UV completions and further assuming weak coupling, by itself, would not improve the bound (1.6). The UV completion may equally well be strongly coupled at the scale $\Lambda_{\rm new}$ or lead to an infinite tower of higher spin states as is required in any tree level completion of gravity such as string theory. We only require that QED minimally coupled to gravity be a good description at low energies and that the Froissart bound in the weak sense $|\mathcal{A}(s,t)| < |s|^2$ is respected at sufficiently large $|s| \to \infty$ (the fact that at low energy another scaling in s is observed is irrelevant). A nonlocal UV completion could in principle violate the latter and would evade these considerations, but would in itself be a startling conclusion.

We begin in Sec. II with a review of the standard discussion of positivity bounds as applied to the low energy gravitational Euler-Heisenberg Lagrangian. In Sec. III we derive the improved positivity bounds for scalar QED, and in Sec. IV we perform the analogous calculation for spinor QED. Most of the calculational details are saved for the Appendixes.

II. BOUNDS FROM EULER-HEISENBERG

In the following we consider the theory of QED minimally coupled to gravity, which is itself a low energy EFT. The action for the fermionic (spinor) QED reads

$$\mathcal{L}_{\rm QED} = \sqrt{-g}\left[\frac{M_{\rm Pl}^2}{2}R - \frac{1}{4}F_{\mu\nu}F^{\mu\nu} - \bar{\psi}(i\not{\nabla} + m)\psi - eA_\mu\bar{\psi}\gamma^\mu\psi\right], \tag{2.1}$$

where ψ is the Dirac field; $\bar{\psi} \equiv \psi^\dagger\gamma^0$, $\not{\nabla} \equiv \gamma^\mu\nabla_\mu$, and $\gamma^\mu = v_a^\mu\gamma^a$ are the gamma matrices; v_μ^a is the vierbein; and ∇ is the covariant derivative with the spin connection (see Appendix B 1). We denote by m and e the electron mass and charge, respectively. When the role of the electron is played by a complex scalar field, the action for scalar QED is then

$$\mathcal{L}_{\rm sQED} = \sqrt{-g}\left[\frac{M_{\rm Pl}^2}{2}R - \frac{1}{4}F_{\mu\nu}F^{\mu\nu} - D_\mu\phi D^\mu\phi^\dagger - m^2\phi\phi^\dagger\right], \tag{2.2}$$

where ϕ is the complex scalar and the gauge-covariant derivative is defined as usual $D_\mu \equiv \partial_\mu - ieA_\mu$. Throughout this work we use mostly plus signature $(-,+,+,+)$.

A. Gravitational Euler-Heisenberg effective field theory

Below the electron mass, we may integrate out the heavy electron from (2.1) and (2.2), respectively. We refer to this as the gravitational Euler-Heisenberg effective field theory. The resulting EFT involves higher derivative interactions between the Maxwell field and graviton and can be parametrized as

$$\begin{aligned} S_{\text{Eul-Heis},1} = \int {\rm d}^4x\sqrt{-g}\Bigg[&\frac{M_{\rm Pl}^2}{2}R - \frac{1}{4}F_{\mu\nu}F^{\mu\nu} + \frac{a_1}{m^4}(F_{\mu\nu}F^{\mu\nu})^2 \\ &+ \frac{a_2}{m^4}(F_{\mu\nu}\tilde{F}^{\mu\nu})^2 + \frac{b_1}{m^2}RF_{\mu\nu}F^{\mu\nu} \\ &+ \frac{b_2}{m^2}R_{\mu\nu}F^{\mu\lambda}F^{\nu}{}_{\lambda} + \frac{b_3}{m^2}R_{\mu\nu\lambda\rho}F^{\mu\nu}F^{\lambda\rho} \\ &+ c_1R^2 + c_2R_{\mu\nu}R^{\mu\nu} + c_3R_{\mu\nu\rho\sigma}R^{\mu\nu\rho\sigma} + \cdots\Bigg], \end{aligned} \tag{2.3}$$

where the ellipses designate higher order operators and where we have defined $\tilde{F}_{\mu\nu} \equiv \varepsilon_{\mu\nu\alpha\beta}F^{\alpha\beta}/2$. The form of these operators is the same independent of whether one starts with the spinor or scalar QED; only the exact values of the coefficients a_i, b_i vary. In turn, the c_i couplings appearing in front of the curvature-squared operators are different. These arise even in the case when electron charge e is zero and encode the backreaction of any matter fields on the metric, more precisely the propagator of the spin-2 state. The couplings c_i thus receive contributions from any matter field coupled to gravity and are not solely determined from our QED EFT. The role of these terms is discussed in more detail in Sec. IV D.

The coefficients for the spinor QED are known to be [33,40]

$$a_1 = \frac{\alpha^2}{90}, \qquad a_2 = \frac{7\alpha^2}{360},$$
$$b_1 = \frac{\alpha}{144\pi}, \qquad b_2 = -\frac{13\alpha}{360\pi}, \qquad b_3 = \frac{\alpha}{360\pi}, \tag{2.4}$$

while for scalar QED the coefficients are [40,55,56]

$$a_1 = \frac{7\alpha^2}{1440}, \qquad a_2 = \frac{\alpha^2}{1440},$$
$$b_1 = -\frac{\alpha}{288\pi}, \quad b_2 = -\frac{\alpha}{360\pi}, \quad b_3 = -\frac{\alpha}{720\pi}, \tag{2.5}$$

where $\alpha = e^2/(4\pi)$ is the fine-structure constant. The action (2.3) can be further simplified by expressing the Riemann tensor in terms of the Weyl tensor C and using the lowest order Einstein equations (i.e., performing a field redefinition). To this order in the EFT, this leads to

$$\mathcal{L}_{\text{Eul-Heis},2} = \sqrt{-g}\left[\frac{M_{\text{Pl}}^2}{2}R - \frac{1}{4}F_{\mu\nu}F^{\mu\nu} + \frac{a_1'}{m^4}(F_{\mu\nu}F^{\mu\nu})^2 + \frac{a_2'}{m^4}(F_{\mu\nu}\tilde{F}^{\mu\nu})^2 + \frac{b_3}{m^2}F_{\mu\nu}F_{\rho\sigma}C^{\mu\nu\rho\sigma}\right], \tag{2.6}$$

where $\tilde{F}_{\mu\nu}$ is the dual field strength tensor and (after setting $c_i = 0$) the new coefficients are[4]

$$a_1' = a_1 + \frac{1}{4}\frac{m^2}{M_{\text{Pl}}^2}b_2 + \frac{1}{2}\frac{m^2}{M_{\text{Pl}}^2}b_3,$$
$$a_2' = a_2 + \frac{1}{4}\frac{m^2}{M_{\text{Pl}}^2}b_2 + \frac{1}{2}\frac{m^2}{M_{\text{Pl}}^2}b_3. \tag{2.7}$$

Notably, both couplings a_i and b_i contribute to the two F^4 terms in the action; it is, however, important to emphasize the difference in their physical origins. For this, let us note that in the gravitational Euler-Heisenberg action (2.6) these arise with different mass scalings in front of the corresponding operators, so that we have

$$\frac{a_i}{m^4} \sim \frac{e^4}{m^4}, \qquad \frac{m^2}{M_{\text{Pl}}^2}\frac{b_i}{m^4} \sim \frac{e^2}{m^2 M_{\text{Pl}}^2}. \tag{2.8}$$

The appearance of the inverse powers of M_{Pl} in the b-terms indicate that the scattering processes leading to the low energy F^4 interactions are different in the two cases. The couplings a_i are generated by four-photon scatterings involving only electron exchange (shown on the first line of Fig. 2 or in the first diagram of Fig. 3). The couplings b_i in turn are generated by gravitational four-photon scattering involving a massless graviton exchange as shown on the second line of Fig. 2 (or in the last three diagrams of Fig. 3).

[4]Note that these relations differ slightly from those given in Eq. (3.4) of [40]. Importantly, there is a sign difference in both b_2 and b_3 due to the fact that the coefficients b_i change sign under the signature change. The numerical factors coincide if one switches the units, e.g., $1/4M_{\text{Pl}}^2 = 4\pi G/2 = 1/2$, since $4\pi G \equiv 1$ in [40].

B. Positivity bounds from the Euler-Heisenberg EFT

The leading contribution to the four-photon $AA \to AA$ scattering amplitude in the gravitational Euler-Heisenberg theory below the electron mass (2.6) comes from the scattering processes shown in Fig. 1. Although not explicit in the diagrams, b_3 enters through a modified graviton-photon-photon vertex. Consistent with the previous literature, we find the following results for the various helicity configurations of the ingoing and outgoing particles (written in an all ingoing convention):

$$\begin{aligned}
\mathcal{A}_{\text{Eul-Heis}}(++++) &= \mathcal{A}_{\text{Eul-Heis}}(----) \\
&= \frac{8(a_1' - a_2')}{m^4}(s^2+t^2+u^2), \\
\mathcal{A}_{\text{Eul-Heis}}(++--) &= \mathcal{A}_{\text{Eul-Heis}}(--++) \\
&= \frac{s^4}{M_{\text{Pl}}^2 stu} + \frac{8(a_1' + a_2')}{m^4}s^2, \\
\mathcal{A}_{\text{Eul-Heis}}(+-+-) &= \mathcal{A}_{\text{Eul-Heis}}(-+-+) \\
&= \frac{t^4}{M_{\text{Pl}}^2 stu} + \frac{8(a_1' + a_2')}{m^4}t^2, \\
\mathcal{A}_{\text{Eul-Heis}}(+--+) &= \mathcal{A}_{\text{Eul-Heis}}(-++-) \\
&= \frac{u^4}{M_{\text{Pl}}^2 stu} + \frac{8(a_1' + a_2')}{m^4}u^2.
\end{aligned} \tag{2.9}$$

The b_3 interaction vertex only contributes to the $\mathcal{A}_{\text{Eul-Heis}}(+++-)$, $\mathcal{A}_{\text{Eul-Heis}}(---+)$, etc., amplitudes as [40]

$$\begin{aligned}
\mathcal{A}_{\text{Eul-Heis}}(+++-) &= \mathcal{A}_{\text{Eul-Heis}}(---+) \\
&= \frac{b_3}{M_{\text{Pl}}^2 m^2}(s^2+t^2+u^2).
\end{aligned} \tag{2.10}$$

These amplitudes respect $s-u$ crossing symmetry in the sense

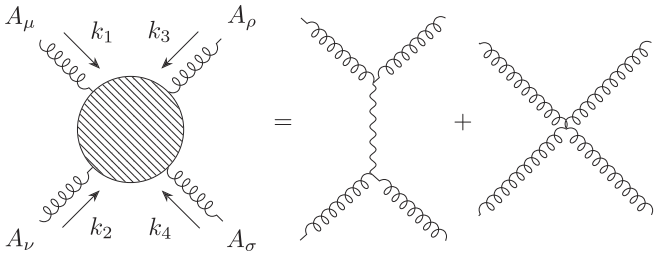

FIG. 1. The $AA \to AA$ t-channel scattering in the gravitational Euler-Heisenberg theory. The wiggly line stands for the vector field A_μ. The exchanged wavy line stands for the graviton $h_{\mu\nu}$.

$$\mathcal{A}(\lambda_1\lambda_2\lambda_3\lambda_4)(s,t,u) = \mathcal{A}(\lambda_1\lambda_4\lambda_3\lambda_2)(u,t,s). \tag{2.11}$$

As expected, the amplitudes (2.9) involve the infamous t-channel pole diverging in the forward limit, thus formally invalidating any analyticity arguments that would lead to the positivity bounds. Interestingly, in [40] it was proven that upon discarding the massless graviton pole and after symmetrizing the scattering amplitudes above, the positivity bounds imply

$$a_1' + a_2' > 0. \tag{2.12}$$

Alternatively, this result may also be obtained by analyzing the elastic amplitude $\mathcal{A}(++--) \equiv \mathcal{A}(++ \to ++)$ alone. Inserting the expressions of the coefficients (2.7) we get

$$a_1 + a_2 + \frac{m^2}{M_{\rm Pl}^2}\left(\frac{b_2}{2} + b_3\right) > 0. \tag{2.13}$$

As discussed earlier, the exact values of the coefficients a_i and b_i are known from the QED EFT (2.6) and are given in Eqs. (2.4) and (2.5). For the scalar QED this implies[5]

$$\frac{e^4}{2880 M_{\rm Pl}^2\pi^2}\left(-2\frac{m^2}{e^2} + M_{\rm Pl}^2\right) > 0, \tag{2.14}$$

while for the spinor QED this leads to

$$\frac{e^4}{5760 M_{\rm Pl}^2\pi^2}\left(-24\frac{m^2}{e^2} + 11 M_{\rm Pl}^2\right) > 0. \tag{2.15}$$

Taking these bounds at their face value one would be tempted to conclude that these imply the weak-gravity type of bounds on the charge-to-mass ratio, i.e., that $e/m \gtrsim \sqrt{2}/M_{\rm Pl}$, which was one of the remarkable points presented in [40]. However, as we shall see below, the previous bounds rely on known positive QED contributions, namely that from the nongravitational electron loop. However, the *raison d'être* of positivity bounds is to probe the unknown UV contributions. Any known contributions from the EFT can and should be removed by means of the improved positivity bounds, as we describe below, before any physical conclusions are derived.

The bounds (2.12) are not the only bounds that may be derived assuming the t-channel pole may be discarded; we may also consider states of indefinite polarization which mix in information about b_3. For instance, taking the incoming polarization state to be $|+\rangle \otimes \frac{1}{\sqrt{2}}(|+\rangle \pm |-\rangle)$ the positivity bound becomes $4(a_1' + a_2') > m^2|b_3|/M_{\rm Pl}^2$. For specific indefinite polarization states corresponding to those that are natural from compactification to 3D, we may then recover, for example, the bounds argued for in [42]. In our current notation these are the statements that

$$4a_1' > \frac{m^2}{M_{\rm Pl}^2}|b_3|, \qquad a_2' > 0, \tag{2.16}$$

which are stronger and therefore include (2.13). Once again, taken at face value for QED minimally coupled to gravity, we would be led to a similar conclusion about the charge-to-mass ratio in order to satisfy them, a conclusion that would be premature.

Before proceeding we note that the bound discussed in [40] has been countered in the case of 3D by the discussion of [43] which makes use of extended positivity bounds of [31], leading to an opposing bound on the charge-to-mass ratio. This parallels some of the discussion in what follows for four dimensions (4D), although we shall make use of the improved positivity bounds which allow us to infer a bound on the cutoff of the EFT and avoid the need to focus on the high powers of s in the expansion of the amplitude.

III. BOUNDS FROM SCALAR QED COUPLED TO GRAVITY

Our goal is to extend the argumentation of the previous section, whereby, instead of applying the positivity bounds to the Euler-Heisenberg Lagrangian, we shall apply them directly to QED minimally coupled to gravity—itself treated as a low energy EFT. The new feature is that the resulting EFT is valid at and above the mass of the electron (up to the EFT cutoff Λ_c), and so we may use the "knowledge" of electron loop contributions to "improve" the positivity bounds. Before we do this we outline in more detail the improved positivity bounds in the next subsection.

A. Improved positivity and dispersion relations

The fixed t dispersion relation for the pole-subtracted amplitude $\tilde{\mathcal{A}}(s,t,u)$ can be written in a maximally s-u crossing symmetric way as

$$\tilde{\mathcal{A}}(s,t,u) = a_1(t) + a_2(t)s + \frac{s^2}{\pi}\int_0^\infty ds' \frac{\mathrm{Disc}_s\mathcal{A}(s',t,u')}{s'^2(s'-s)} + \frac{u^2}{\pi}\int_0^\infty du' \frac{\mathrm{Disc}_u\mathcal{A}(s',t,u')}{u'^2(u'-u)}, \tag{3.1}$$

where $s' + u' + t = 0$ for massless photons. Assuming that the unknown UV completion at energies well above the electron mass has the Froissart-like behavior $\lim_{|s|\to\infty}\mathcal{A}_{\rm UV}(s,t)/s^2 = 0$, Cauchy's theorem may be applied to $\partial_s^2\mathcal{A}(s,t)$, with a vanishing contribution from the contour at infinity, from which the subtraction terms $a_1(t) + a_2(t)s$ arise. The discontinuities in the dispersion

[5]The relations (2.14) and (2.15) are given for $c_i = 0$, whereas [40] also accounts for the nonzero c_i. The implications of nonzero c_i, which contribute at order $1/M_{\rm Pl}^4$ in the amplitudes, are discussed in Sec. IV D.

relation above are with respect to the Mandelstam variable that corresponds to the center of mass (CoM) energy squared of either the s or the u channel,

$$2i\mathrm{Disc}_s\mathcal{A}(s,t,u) \equiv \mathcal{A}(s+i\epsilon,t,u=-s-t-i\epsilon) - \mathcal{A}(s-i\epsilon,t,u=-s-t+i\epsilon) \tag{3.2}$$

and

$$2i\mathrm{Disc}_u\mathcal{A}(s,t,u) \equiv \mathcal{A}(s=-u-t-i\epsilon,t,u+i\epsilon) - \mathcal{A}(s=-u-t+i\epsilon,t,u-i\epsilon). \tag{3.3}$$

Explicitly, crossing symmetry implies that

$$\mathcal{A}_{\lambda_1\lambda_2\to\lambda_3\lambda_4}(s,0,u) = \mathcal{A}_{\lambda_1-\lambda_4\to\lambda_3-\lambda_2}(u,0,s), \tag{3.4}$$

and so the left-hand u-channel discontinuity is defined so that

$$\begin{aligned}\mathrm{Disc}_u\mathcal{A}_{\lambda_1\lambda_2\to\lambda_3\lambda_4}(s,0,u) &= \mathrm{Disc}_u\mathcal{A}_{\lambda_1-\lambda_4\to\lambda_3-\lambda_2}(u,0,s)\\ &= [\mathrm{Disc}_s\mathcal{A}_{\lambda_1-\lambda_4\to\lambda_3-\lambda_2}(s,0,u)]_{u\leftrightarrow s},\end{aligned} \tag{3.5}$$

which is just the standard right-hand discontinuity of the crossed process $A+\bar{D}\to C+\bar{B}$ (associated with $A+B\to C+D$). The physical discontinuities are therefore positive in the forward limit for elastic scattering by unitarity on both the right-hand and left-hand cuts, leading to the forward limit positivity bound,

$$\partial_s^2\tilde{\mathcal{A}}(0,0,0) = \frac{2}{\pi}\int_0^\infty \mathrm{d}s'\frac{\mathrm{Disc}_s\mathcal{A}(s',0,u')}{s'^3} + \frac{2}{\pi}\int_0^\infty \mathrm{d}u'\frac{\mathrm{Disc}_u\mathcal{A}(s',0,u')}{u'^3} > 0. \tag{3.6}$$

This positivity bound can be improved by then subtracting a known positive contribution to the discontinuities from both sides of the dispersion relation. This discontinuity can be computed in the EFT (e.g., QED in our case), giving a result that can be trusted well below its cutoff scale Λ_c; hence the integrals over s' and u' must be cut off at $\epsilon^2\Lambda_c^2$ with $\epsilon \ll 1$. This can then be achieved by a split

$$\begin{aligned}\mathrm{Disc}_s\mathcal{A}(s',0,u') &= \mathrm{Disc}_s\mathcal{A}(s',0,u')\theta(\epsilon^2\Lambda_c^2-s) + \mathrm{Disc}_s\mathcal{A}(s',0,u')\theta(s-\epsilon^2\Lambda_c^2),\\ \mathrm{Disc}_u\mathcal{A}(s',0,u') &= \mathrm{Disc}_u\mathcal{A}(s',0,u')\theta(\epsilon^2\Lambda_c^2-u) + \mathrm{Disc}_u\mathcal{A}(s',0,u')\theta(u-\epsilon^2\Lambda_c^2),\end{aligned} \tag{3.7}$$

where the first term on the right-hand side (RHS) is regarded as the "known" part of the discontinuity, and both known and unknown pieces are positive separately. We may then define the improved scattering amplitude $\mathcal{A}^{\mathrm{imp}}(s,t,u)$ via [9,10]

$$\mathcal{A}^{\mathrm{imp}}(s,t,u) \equiv \tilde{\mathcal{A}}(s,t,u) - \frac{s^2}{\pi}\int_0^{\epsilon^2\Lambda_c^2}\mathrm{d}s'\frac{\mathrm{Disc}_s\mathcal{A}(s',t,u')}{s'^2(s'-s)} - \frac{u^2}{\pi}\int_0^{\epsilon^2\Lambda_c^2}\mathrm{d}u'\frac{\mathrm{Disc}_u\mathcal{A}(s',t,u')}{u'^2(u'-u)}. \tag{3.8}$$

Crucially $\mathcal{A}^{\mathrm{imp}}(s,t,u)$ has the same analytic structure as $\tilde{\mathcal{A}}(s,t,u)$ except that by construction the branch cuts now start at $s'=\epsilon^2\Lambda_c^2$ and $u'=\epsilon^2\Lambda_c^2$. We may then derive improved positivity bounds from $\tilde{\mathcal{A}}^{\mathrm{imp}}(s,t,u)$ in the same manner in which they are derived from $\mathcal{A}^{\mathrm{imp}}(s,t,u)$, in particular leading to the forward limit bound

$$\partial_s^2\mathcal{A}^{\mathrm{imp}}(0,0,0) = \partial_s^2\tilde{\mathcal{A}}(0,0,0) - \frac{2}{\pi}\int_0^{\epsilon^2\Lambda_c^2}\mathrm{d}s'\frac{\mathrm{Disc}_s\mathcal{A}(s',0,u')}{s'^3} - \frac{2}{\pi}\int_0^{\epsilon^2\Lambda_c^2}\mathrm{d}u'\frac{\mathrm{Disc}_u\mathcal{A}(s',0,u')}{u'^3} > 0. \tag{3.9}$$

To proceed we need to know not only the low energy expansion of the amplitude but also the low energy discontinuities. These receive contributions from both nongravitational diagrams and gravitational ones, and we shall deal with each of these in turn.

B. Discontinuities of nongravitational diagrams

The full set of diagrams for scalar QED that contribute to the one-loop four-photon amplitude to order $1/M_{\mathrm{Pl}}^2$, including graviton exchange, are given in Fig. 2. In general the discontinuities can be inferred by unitarity cuts; however, we choose to derive them directly from the amplitudes provided in Appendix A. The discontinuities are calculated within the domain relevant to the dispersion relation, namely the physical region which for, e.g., $\mathrm{Disc}_s\mathcal{A}(s',0,u')$, is $s'\geq 0$. In general it is necessary to keep track of both the discontinuities of the original process $A+B\to C+D$ and the crossed process $A+\bar{D}\to C+\bar{B}$. We use the results and notation of Appendix A 4. Focusing for now on the nongravitational contributions (i.e., those with no internal graviton lines), we denote by $\mathcal{A}_n$ the contributions to the amplitude arising from diagrams with n internal ϕ propagators. For scalar QED the relevant discontinuities from individual Feynman diagrams are, respectively,

(i) For two internal lines,

$$\mathrm{Disc}_s\mathcal{A}_2(s,0,u) = \frac{e^4}{4\pi}\varepsilon_{12}\varepsilon_{34}\sqrt{\frac{s-4m^2}{s}}\theta(s-4m^2);$$

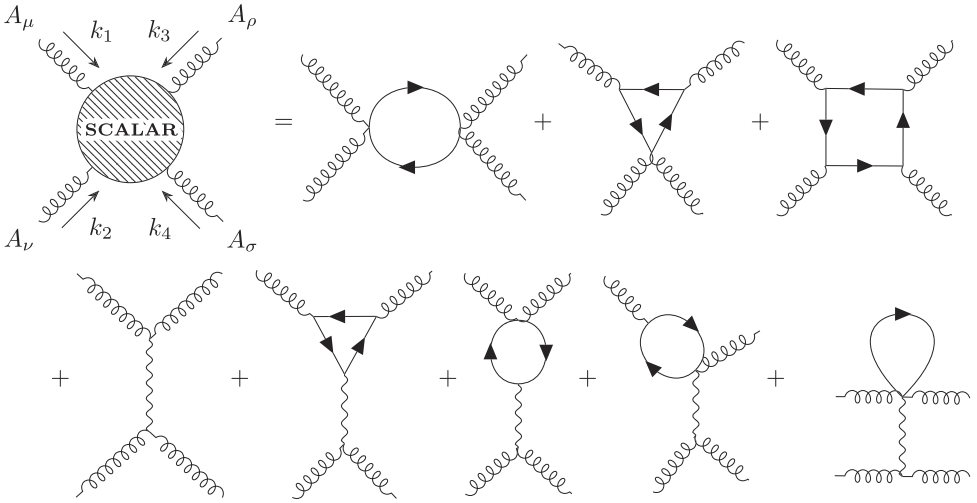

FIG. 2. The $AA \to AA$ scattering in scalar QED due to nongravitational interactions (first line) and gravitational interactions to order $1/M_{\rm Pl}^2$ (second line). The wiggly line stands for the vector field A_μ, and the solid line stands for the scalar field ϕ. The arrows depict the direction of the charge flow. We do not show all the crossed versions of the diagrams.

(ii) For three internal lines,

$$\mathrm{Disc}_s\mathcal{A}_3(s,0,u) = -\frac{e^4}{\pi}\varepsilon_{12}\varepsilon_{34}\left(\frac{\sqrt{s(s-4m^2)}+2m^2\ln\left(\frac{2m^2}{s-2m^2+\sqrt{s(s-4m^2)}}\right)}{2s}\right)\theta(s-4m^2); \tag{3.10}$$

(iii) And finally for four internal lines,

$$\begin{aligned}\mathrm{Disc}_s\mathcal{A}_4(s,0,u) = \frac{e^4}{8\pi s^2}\Bigg\{&\sqrt{s(s-4m^2)}(s+2m^2) - 4sm^2\left(\ln 4 + 3\ln\frac{s}{m^2} - 4\ln\frac{s-\sqrt{s(s-4m^2)}}{m^2}\right)\\ &- 2m^2(m^2+4s)\ln\left(1-\sqrt{\frac{s-4m^2}{s}}\right) + 2m^4\ln\left(-3-\sqrt{\frac{s-4m^2}{s}}+\frac{s}{m^2}+\frac{\sqrt{s(s-4m^2)}}{m^2}\right)\Bigg\}\\ &\times\theta(s-4m^2)\times(\varepsilon_{12}\varepsilon_{34}+\varepsilon_{14}\varepsilon_{23}+\varepsilon_{13}\varepsilon_{24}).\end{aligned}$$

In all cases the associated u-channel discontinuities can be inferred from

$$\mathrm{Disc}_u\mathcal{A}_n(s,0,u) = [\mathrm{Disc}_s\mathcal{A}_n(s,0,u)]_{s\leftrightarrow u,2\leftrightarrow 4}. \tag{3.11}$$

The total amplitude is the sum of all contributions $\mathcal{A}(s,t,u) = Z_A^2\mathcal{A}_{\rm tree}(s,t,u) + \mathcal{A}_2(s,t,u) + \mathcal{A}_3(s,t,u) + \mathcal{A}_4(s,t,u)$, accounting for wave function renormalization, and so the discontinuities combine accordingly.

C. Checking against the dispersion relation

As a simple consistency check, we can verify expression (3.6) for the second derivative of the dispersion relation. Direct integration of the discontinuities gives

$$\frac{2}{\pi}\int_0^\infty \mathrm{d}s'\frac{\mathrm{Disc}_s\mathcal{A}(s',0,u')}{s'^3} + \frac{2}{\pi}\int_0^\infty \mathrm{d}u'\frac{\mathrm{Disc}_u\mathcal{A}(s',0,u')}{u'^3} = \frac{e^4}{240\pi^2m^4}\left(\varepsilon_{12}\varepsilon_{34}+\varepsilon_{14}\varepsilon_{23}+\frac{1}{3}\varepsilon_{13}\varepsilon_{24}\right), \tag{3.12}$$

whereas taking the derivative directly of the nongravitational amplitude gives

$$\partial_s^2\tilde{\mathcal{A}}(0,0,0) = \frac{e^4}{240\pi^2m^4}\left(\varepsilon_{12}\varepsilon_{34}+\varepsilon_{14}\varepsilon_{23}+\frac{1}{3}\varepsilon_{13}\varepsilon_{24}\right), \tag{3.13}$$

confirming the validity of the dispersion relation with two subtractions in the absence of gravity.

D. Discontinuities of gravitational diagrams

The gravitational diagrams for scalar QED that contribute to order $1/M_{\rm Pl}^2$ are computed in Appendix A 5 and contain individual Feynman diagram contributions labeled $\mathfrak{a}$, $\mathfrak{b}$, $\mathfrak{c}$, $\mathfrak{d}$ in Fig. 6. We find that the type $\mathfrak{c}$, $\mathfrak{d}$ diagrams do not produce any discontinuity. This is because the denominator of the loop integrand has a strictly positive real part. We find the $\mathfrak{b}$ type diagrams also have zero imaginary part, so we can focus solely on the type $\mathfrak{a}$ diagrams. We shall define the following scattering configurations:

$$\begin{aligned}\text{Configuration I}&: ++--\equiv ++\to ++\\ \text{Configuration II}&: +--+\equiv +-\to +-\\ \text{Configuration III}&: +-+-\equiv +-\to -+\end{aligned}$$

and focus only on these for illustrative purposes. The first two configurations are elastic so positivity bounds apply to them.

1. Configuration I

The loop diagrams with one graviton exchange have the following discontinuities:

$$\text{Disc}_s\mathcal{A}_{\rm I}(s,0,u)=0, \tag{3.14}$$

$$\begin{aligned}&\text{Disc}_u\mathcal{A}_{\rm I}(s,0,u)\\ &=\frac{e^2}{24\pi M_{\rm Pl}^2 u}\left((10m^2-u)\sqrt{u(u-4m^2)}\right.\\ &\quad\left.-24m^4\tanh^{-1}\left(\sqrt{\frac{u-4m^2}{u}}\right)\right)\theta(u-4m^2).\end{aligned} \tag{3.15}$$

Note that this discontinuity is strictly negative in the physical region. This does not contradict unitarity since this is a perturbative gravitational correction to an already positive nongravitational discontinuity.

2. Configuration II

$$\begin{aligned}&\text{Disc}_s\mathcal{A}_{\rm II}(s,0,u)\\ &=\frac{e^2}{24\pi M_{\rm Pl}^2 s}\left((10m^2-s)\sqrt{s(s-4m^2)}\right.\\ &\quad\left.-24m^4\tanh^{-1}\left(\sqrt{\frac{s-4m^2}{s}}\right)\right)\theta(s-4m^2).\end{aligned} \tag{3.16}$$

Note that this discontinuity is also strictly negative, while the u-channel contribution cancels,

$$\text{Disc}_u\mathcal{A}_{\rm II}(s,0,u)=0. \tag{3.17}$$

3. Configuration III

The forward limit of this helicity configuration has zero discontinuity which agrees with the gravitational Euler-Heisenberg result as the gravitational part of the amplitude in this configuration is zero in the forward limit.

E. Checking against the dispersion relation

If it were the case that QED coupled to gravity still respected the Jin-Martin version of the Froissart bound to the one-loop level, i.e., $|A(s,t)|<|s|^2$, then it would still be possible to write a dispersion relation for the scattering amplitude with two subtractions. Furthermore, if this were the case it would be possible to use the improved positivity bound to remove even the gravitational contributions. Fortunately this is not the case, and it is this very fact that will lead to our central result. For scalar QED in configuration I the gravitational contribution to the amplitude gives

$$\mathcal{A}_{\rm I}''(0)=-\frac{e^2}{90\pi^2m^2M_{\rm Pl}^2}, \tag{3.18}$$

whereas the usual dispersion integrals give

$$\frac{2}{\pi}\int_0^\infty ds'\,\frac{\text{Disc}_s\mathcal{A}_{\rm I}(s',0,u')}{s'^3}+(s\leftrightarrow u)=-\frac{e^2}{180m^2\pi^2M_{\rm Pl}^2}. \tag{3.19}$$

By contrast higher derivatives of the dispersion relation do match, which is to be expected since we *can* write a dispersion relation for the one-loop gravitational contribution with three subtractions, and for any $n\geq 3$, so we do expect the following to hold:

$$\begin{aligned}\partial_s^n\mathcal{A}(0,0,0)=&\frac{n!}{\pi}\int_0^\infty ds'\,\frac{\text{Disc}_s\mathcal{A}(s',0,u')}{s'^{n+1}}\\ &+\frac{(-1)^n n!}{\pi}\int du'\,\frac{\text{Disc}_u\mathcal{A}(s',0,u')}{u'^{n+1}}.\end{aligned} \tag{3.20}$$

Indeed, for configuration I the integrals on the RHS give

$$\begin{aligned}&0+\frac{(-1)^n n!}{\pi}\int du'\,\frac{\text{Disc}_u\mathcal{A}_{\rm I}(s',0,u')}{u'^{n+1}}\\ &\quad=\frac{e^2(-1)^n 2^{-2(n+1)}n!\csc(\pi n)}{\sqrt{\pi}M_{\rm Pl}^2m^{2(n-1)}(n+1)\Gamma(2-n)\Gamma(n+\frac{3}{2})},\end{aligned} \tag{3.21}$$

whereas from taking derivatives of the amplitude for the left-hand side (LHS) we obtain

$$\mathcal{A}_{\rm I}^{(n)}(0,0,0)=\frac{e^2(-1)^{n+1}\Gamma(n-1)\Gamma(n+1)\Gamma(n+2)}{M_{\rm Pl}^2 m^{2(n-1)}\pi^2(n+1)\Gamma(2n+3)}, \tag{3.22}$$

which is, in fact, equal to the dispersion integral result, so the dispersion relation holds for all $n \geq 3$.

It is worth stressing that the fact that the low energy amplitude computed within the EFT does not satisfy the Jin-Martin version of the Froissart bound at the one-loop level does not in any way imply that the full UV amplitude would itself need to violate Froissart. It is indeed inevitable in an EFT that amplitudes computed to finite order in an energy expansion grow "too fast," indicating only the breakdown of the effective theory. It is precisely because of this fact that positivity bounds are so powerful.

F. Improved positivity bounds

We now have all the essential ingredients needed to derive our main result. Assuming that the improved positivity bounds can be applied with the t-channel pole discarded, then the fact that the nongravitational amplitudes for QED do respect Froissart at one-loop, but the gravitational corrections (as computed within the QED EFT) do not, will enforce a nontrivial bound on the cutoff of the low energy effective theory. Let us focus on the configuration I amplitude which is elastic in polarizations $++ \to ++$.

The s-channel integral is

$$\begin{aligned}\frac{2}{\pi}\int_{4m^2}^{\epsilon^2\Lambda_c^2} ds \frac{\mathrm{Disc}_s\mathcal{A}(s,0,u)}{s^3}=\frac{2e^2}{\pi^2}\int_{4m^2}^{\epsilon^2\Lambda_c^2}\frac{ds}{s^3}\Bigg[&\frac{e^2}{4}\sqrt{\frac{s-4m^2}{s}}-e^2\left(\frac{\sqrt{s(s-4m^2)}+2m^2\ln\left(\frac{2m^2}{s-2m^2+\sqrt{s(s-4m^2)}}\right)}{2s}\right)\\&+\frac{e^2}{4s^2}\Bigg\{\sqrt{s(s-4m^2)}(s+2m^2)-4sm^2\left(\ln 4+3\ln\frac{s}{m^2}-4\ln\frac{s-\sqrt{s(s-4m^2)}}{m^2}\right)\\&-2m^2(m^2+4s)\ln\left(1-\sqrt{\frac{s-4m^2}{s}}\right)+2m^4\ln\left(-3-\sqrt{\frac{s-4m^2}{s}}+\frac{s}{m^2}+\frac{\sqrt{s(s-4m^2)}}{m^2}\right)\Bigg\}\Bigg],\end{aligned} \tag{3.23}$$

while the u-channel integral is

$$\begin{aligned}\frac{2}{\pi}\int_{4m^2}^{\epsilon^2\Lambda_c^2} du \frac{\mathrm{Disc}_u\mathcal{A}(s,0,u)}{u^3}=\frac{2e^2}{\pi^2}\int_{4m^2}^{\epsilon^2\Lambda_c^2}\frac{du}{u^3}\Bigg[&\frac{e^2}{4u^2}\Bigg\{\sqrt{u(u-4m^2)}(u+2m^2)-4um^2\left(\ln 4+3\ln\frac{u}{m^2}-4\ln\frac{u-\sqrt{u(u-4m^2)}}{m^2}\right)\\&-2m^2(m^2+4u)\ln\left(1-\sqrt{\frac{u-4m^2}{u}}\right)+2m^4\ln\left(-3-\sqrt{\frac{u-4m^2}{u}}+\frac{u}{m^2}+\frac{\sqrt{u(u-4m^2)}}{m^2}\right)\Bigg\}\\&+\frac{1}{24M_{\rm Pl}^2 u}\left((10m^2-u)\sqrt{u(u-4m^2)}-24m^4\tanh^{-1}\left(\sqrt{\frac{u-4m^2}{u}}\right)\right)\Bigg].\end{aligned} \tag{3.24}$$

Inserting the discontinuities into the improved positivity bounds and expanding the integrals given the necessary assumption $m \ll \epsilon\Lambda_c$ lead to

$$\begin{aligned}&0<\partial_s^2\tilde{\mathcal{A}}(0,0,0)-\frac{2}{\pi}\int_0^{\epsilon^2\Lambda_c^2}ds'\frac{\mathrm{Disc}_s\mathcal{A}(s',0,u')}{s'^3}-\frac{2}{\pi}\int_0^{\epsilon^2\Lambda_c^2}du'\frac{\mathrm{Disc}_u\mathcal{A}(s',0,u')}{u'^3},\\&0<\frac{e^4}{4\pi^2\Lambda_c^4\epsilon^4}+\frac{e^2m^2}{2\pi^2M_{\rm Pl}^2\Lambda_c^4\epsilon^4}-\frac{e^2}{180\pi^2m^2M_{\rm Pl}^2}-\frac{e^2}{12\pi^2M_{\rm Pl}^2\Lambda_c^2\epsilon^2}+\cdots.\end{aligned} \tag{3.25}$$

Given the assumed EFT hierarchy $m \ll \epsilon\Lambda_c \ll M_{\rm Pl}$ it is sufficient to approximate this as

$$\frac{e^4}{4\pi^2\epsilon^4\Lambda_c^4}-\frac{e^2}{180\pi^2m^2M_{\rm Pl}^2}>0. \tag{3.26}$$

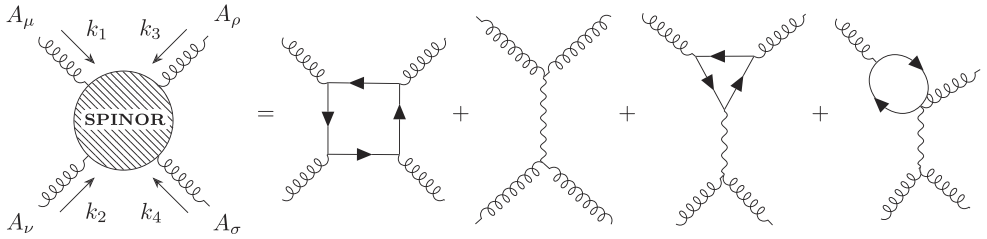

FIG. 3. The $AA \to AA$ scattering in spinor QED due to nongravitational interactions (first term) and gravitational interactions to order $1/M_{\rm Pl}^2$ (remaining terms). The wiggly line stands for the vector field A_μ, and the solid line stands for the fermion ψ. The arrows depict the direction of the charge flow. We do not show all the crossed versions of the diagrams.

The first term is the contribution from nongravitational diagrams which in the absence of gravity can be removed by sending $\Lambda_c \to \infty$, reflecting the statement that QED in flat space automatically satisfies positivity bounds to one-loop. The second term is the distinctively negative gravitational contribution which arises from the non-Froissart growth of the one-loop amplitudes.[6] This positivity bound may be most cleanly interpreted as a bound on the cutoff of the effective theory:

$$\epsilon\Lambda_c \lesssim (emM_{\rm Pl})^{1/2}, \tag{3.27}$$

which is to say that if we take the positivity bound with t-channel pole discarded seriously, QED cannot be minimally coupled to gravity without introducing new physics at or below the scale $\Lambda_{\rm new} \sim (emM_{\rm Pl})^{1/2}$. This is significantly lower than the scale $eM_{\rm Pl}$ implied by the weak gravity conjecture [54], and indeed by the Euler-Heisenberg bounds derived in Sec. II B. The strength of this result is due to the fact that we can remove the known QED contributions to the positivity bounds from the electron loops, up to the cutoff scale $\epsilon\Lambda_c$, giving us a much more constraining condition. This result exactly parallels similar conclusions derived for toy scalar field theories coupled to gravity in a previous work [37]. The present result is, however, cleaner since (a) we do not rely on spectator fields, (b) the form of the QED Lagrangian is more strongly constrained by gauge invariance, and (c) we make no assumption on the types of operators that would arise at the cutoff. Furthermore, if one would possess any additional knowledge about the UV completion of QED minimally coupled to gravity beyond the cutoff Λ_c up to some higher cutoff scale $\Lambda_c' > \Lambda_c$, one could similarly repeat the procedure of the improved positivity bounds up to this new scale. In particular, one could calculate the improved amplitude as in Eq. (3.8) integrating over the discontinuities up to $\epsilon^2\Lambda_c'^2$ and including all the new contributions coming from this new physics to the scattering amplitude $\tilde{\mathcal{A}}(s,t,u)$. In the absence of any such knowledge about the nature of the UV completion, the bound (3.26) is, however, the most generic result. Finally, when the inequality (3.26) comes close to being saturated, we should also worry about higher order corrections in $1/M_{\rm Pl}^2$. These will be considered in Sec. IV D.

IV. BOUNDS FROM SPINOR QED COUPLED TO GRAVITY

The discussion for spinor QED closely parallels that for the scalar QED with the only difference being numerical factors. We sketch the essential arguments leaving the amplitude calculation details to Appendix B. The number of diagrams contributing to the four-photon amplitude at one-loop level and to order $1/M_{\rm Pl}^2$ is significantly fewer as seen in Fig. 3.

A. Discontinuities of nongravitational diagrams

As shown in Fig. 3 the only nongravitational diagram is the "box" diagram. The relevant amplitude discontinuities are given in Appendix B 3 in the s and u channels. For the first two polarization configurations they are, respectively,

$$\mathrm{Disc}_s\mathcal{A}^{\rm I}_{\rm box} = \frac{e^4\pi\theta(s-4m^2)(s-2m^2)}{2\pi^2 s^2}\left(\sqrt{s(s-4m^2)} - 2m^2\log\left(\frac{s-\sqrt{s(s-4m^2)}}{s+\sqrt{s(s-4m^2)}}\right)\right),$$

$$\mathrm{Disc}_u\mathcal{A}^{\rm I}_{\rm box} = \frac{e^4\pi\theta(u-4m^2)}{2\pi^2 u^2}\left(2(-m^2-u)\sqrt{u(u-4m^2)} + (4m^4-2m^2u-u^2)\log\left(\frac{u-\sqrt{u(u-4m^2)}}{u+\sqrt{u(u-4m^2)}}\right)\right),$$

and

[6]We stress again that this does not imply that the UV amplitudes violate the weak Froissart bound $|\mathcal{A}(s,t)| < |s|^2$.

$$\mathrm{Disc}_s\mathcal{A}^{\mathrm{II}}_{\mathrm{box}} = \frac{e^4\pi\theta(s-4m^2)}{2\pi^2 s^2}\left(2(-m^2-s)\sqrt{s(s-4m^2)} + (4m^4-2m^2s-s^2)\log\left(\frac{s-\sqrt{s(s-4m^2)}}{s+\sqrt{s(s-4m^2)}}\right)\right),$$

$$\mathrm{Disc}_u\mathcal{A}^{\mathrm{II}}_{\mathrm{box}} = \frac{e^4\pi\theta(u-4m^2)(u-2m^2)}{2\pi^2 u^2}\left(\sqrt{u(u-4m^2)} - 2m^2\log\left(\frac{u-\sqrt{u(u-4m^2)}}{u+\sqrt{u(u-4m^2)}}\right)\right).$$

All the above discontinuities are positive as required by unitarity. We may confirm the validity of the dispersion relation with two subtractions by demonstrating that

$$\partial_s^2\tilde{\mathcal{A}}(0,0,0) = \frac{2}{\pi}\int_0^\infty \mathrm{d}s'\frac{\mathrm{Disc}_s\mathcal{A}(s',0,u')}{s'^3} + \frac{2}{\pi}\int_0^\infty \mathrm{d}u'\frac{\mathrm{Disc}_u\mathcal{A}(s',0,u')}{u'^3} = \frac{11e^4}{360\pi^2m^4}, \tag{4.1}$$

as required, confirming the discontinuities above for both chosen helicity configurations.

B. Discontinuities of gravitational diagrams

For spinor QED the only gravitational discontinuities come from the type **a** diagrams. The discontinuities of these diagrams are negative and are given by

$$\mathrm{Disc}_u\mathcal{A}^{\mathrm{I}} = -\frac{e^2}{6\pi M_{\mathrm{Pl}}^2 u}\theta(u-4m^2)\left((5m^2+u)\sqrt{u(u-4m^2)} + 3m^2(2m^2+u)\log\left(\frac{u-\sqrt{u(u-4m^2)}}{u+\sqrt{u(u-4m^2)}}\right)\right),$$

$$\mathrm{Disc}_s\mathcal{A}^{\mathrm{I}} = 0,$$

$$\mathrm{Disc}_s\mathcal{A}^{\mathrm{II}} = -\frac{e^2}{6\pi M_{\mathrm{Pl}}^2 s}\theta(s-4m^2)\left((5m^2+s)\sqrt{s(s-4m^2)} + 3m^2(2m^2+s)\log\left(\frac{s-\sqrt{s(s-4m^2)}}{s+\sqrt{s(s-4m^2)}}\right)\right),$$

$$\mathrm{Disc}_u\mathcal{A}^{\mathrm{II}} = 0.$$

As before the negativity of these discontinuities is not in contradiction with unitarity since these are M_{Pl}^2 suppressed corrections to the positive nongravitational discontinuities. Here again, one can explicitly check that this discontinuity is consistent with the relation inferred from the dispersion relation with three subtractions.

C. Improved positivity bounds

Focusing now on the scattering configuration I, the improved positivity bound is [expanding the integrals to next-to-next-to-leading order in powers of $m/(\epsilon\Lambda_c)$],

$$\begin{aligned}
0 &< \partial_s^2\tilde{\mathcal{A}}^{\mathrm{I}}(0,0,0) - \frac{2}{\pi}\int_0^{\epsilon^2\Lambda_c^2}\mathrm{d}s'\frac{\mathrm{Disc}_s\mathcal{A}^{\mathrm{I}}(s',0,u')}{s'^3} - \frac{2}{\pi}\int_0^{\epsilon^2\Lambda_c^2}\mathrm{d}u'\frac{\mathrm{Disc}_u\mathcal{A}^{\mathrm{I}}(s',0,u')}{u'^3},\\
0 &< \frac{11e^4}{360\pi^2m^4} - \frac{11e^2}{180\pi^2m^2M_{\mathrm{Pl}}^2} - \frac{2}{\pi}\int_0^{\epsilon^2\Lambda_c^2}\mathrm{d}s'\frac{\mathrm{Disc}_s\mathcal{A}^{\mathrm{I}}(s',0,u')}{s'^3} - \frac{2}{\pi}\int_0^{\epsilon^2\Lambda_c^2}\mathrm{d}u'\frac{\mathrm{Disc}_u\mathcal{A}^{\mathrm{I}}(s',0,u')}{u'^3},\\
0 &< -\frac{11e^2}{360\pi^2m^2M_{\mathrm{Pl}}^2} - \frac{e^2}{3\pi^2\Lambda^2M_{\mathrm{Pl}}^2} - \frac{e^4}{4\pi^2\Lambda^4} - \frac{e^2m^2}{4\pi^2\Lambda^4M_{\mathrm{Pl}}^2} + \frac{e^4}{\pi^2\Lambda^4}\ln\frac{\Lambda}{m} + \frac{e^2m^2}{\pi^2\Lambda^4M_{\mathrm{Pl}}^2}\ln\frac{\Lambda}{m},
\end{aligned} \tag{4.2}$$

where $\Lambda = \epsilon\Lambda_c$. Once again focusing on the EFT hierarchy $m \ll \epsilon\Lambda_c \ll M_{\mathrm{Pl}}$ this is effectively

$$\frac{e^4}{\pi^2\Lambda^4}\left(\ln\frac{\Lambda}{m} - \frac{1}{4}\right) - \frac{11e^2}{360\pi^2m^2M_{\mathrm{Pl}}^2} > 0. \tag{4.3}$$

As before, without gravity the bound is trivially satisfied, and in the presence of gravity the bound is violated if the cutoff is taken to infinity. If, however, the cutoff scale is taken below

$$\epsilon\Lambda_c \lesssim (emM_{\mathrm{Pl}})^{1/2}, \tag{4.4}$$

positivity is respected. Up to numerical factors this is essentially the same order as the bound derived in scalar QED and suggests a universal result.

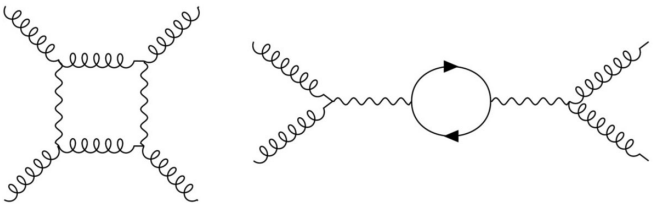

FIG. 4. Example gravitational contributions at order $1/M_{\rm Pl}^4$.

D. Higher order gravitational contributions

Up to now, we have only considered the gravitational corrections to scattering amplitudes up to order $1/M_{\rm Pl}^2$ on the grounds that these dominate. Given the results of the improved positivity bounds, it would be remiss not to address whether higher order corrections, specifically the next ones at order $1/M_{\rm Pl}^4$, could rescue positivity without the need for the low cutoff (4.4). Indeed, as noted already in [40] this is in principle possible. In the context of the improved positivity bounds derived here we can show that this actually leads to equally strong implications. Example Feynman diagrams at this order are given in Fig. 4. They contain no electromagnetic vertices and therefore do not vanish as $e \to 0$. Indeed, any matter species, even uncharged, will give similar contributions. Furthermore these amplitudes are logarithmically divergent within 4D QED minimally coupled to gravity, necessitating the need to add curvature square operators in the actions (2.1) and (2.2) whose coefficients can only be determined by matching onto an unknown UV completion. When included in the amplitude, the improved positivity bounds for spinor QED become

$$\frac{e^4}{\pi^2\Lambda^4}\left(\ln\frac{\Lambda}{m}-\frac{1}{4}\right)-\frac{11e^2}{360\pi^2m^2M_{\rm Pl}^2}-\frac{B}{M_{\rm Pl}^4}\ln\left(\frac{\Lambda}{m}\right)+\frac{\gamma_m}{M_{\rm Pl}^4}>0, \tag{4.5}$$

with a similar expression for scalar QED. Here B is a known positive $\mathcal{O}(1)$ coefficient determined from the positive discontinuities of the diagrams in Fig. 4, and γ_m is an unknown matching coefficient accounting for the curvature square types of operators which needed to be added to the actions (2.1) defined for convenience[7] at a fixed renormalization group (RG) scale $\mu \sim m$. The logarithmic Λ dependence of the B term arises, as in the first term, from the application of the improved bounds which removes the branch cut up to the scale $s' \sim \Lambda^2$. We now see that in principle there is another solution to maintain positivity, other than that of (4.4). Indeed, assuming $\Lambda \gg (emM_{\rm Pl})^{1/2}$ then (4.5) effectively becomes

$$-\frac{11e^2}{360\pi^2m^2M_{\rm Pl}^2}+\frac{\gamma_\Lambda}{M_{\rm Pl}^4}>0. \tag{4.6}$$

Now if γ_Λ is order unity, then (4.6) amounts to a bound of the form $m \gtrsim eM_{\rm Pl}$, in complete opposition to what is anticipated from the weak gravity conjecture. This is, of course, because we are trying to maintain positivity with terms which are higher order in $1/M_{\rm Pl}$ rather than lower order. A similar conclusion was made in the 3D case in [43]. Unlike the situation in 3D, however, we cannot add additional uncharged light states to remove this tension. That is because in 3D the R^2 terms do not need renormalization and any matter fields, even uncharged, contribute to them as $\Delta S \sim \int {\rm d}^3x\sqrt{-g}R^2/m$. Thus by including very light uncharged fields, such as the neutrino, we can maintain overall positivity without needing to satisfy $m \gtrsim eM_{\rm Pl}$.

Returning to four dimensions, more generally we should account for the role of larger γ_Λ which cannot be determined within the QED EFT. The typical expectation for the magnitude of γ_Λ is of order the number of fields N_* that lie below the Planck scale since every matter field contributes a term of this form on integrating out. Then the improved positivity bound (4.6) can be satisfied provided

$$m \gtrsim \frac{eM_{\rm Pl}}{\sqrt{N_*}}. \tag{4.7}$$

In particular, for a weakly coupled UV completion in which new massive spin 2 and higher states arise at a scale M_s, for which $M_{\rm Pl}^2 = M_s^2/g_s^2$, then the scale expected for $\gamma_{\rm UV}$ is $\gamma_{\rm UV} \sim M_{\rm Pl}^2/M_s^2 \sim 1/g_s^2 \gg 1$. In this case (4.6) amounts to

$$m \gtrsim eM_s. \tag{4.8}$$

Unless e is extremely small for *every* charged states in the theory, both of the bounds (4.7) and (4.8) are unreasonable constraints on theories of interest, and so we do not consider this "resolution" to maintain positivity as a meaningful solution. Furthermore they stand in clear opposition to the expectations from weak gravity conjecture [54].

V. DISCUSSION

In this article we have considered whether QED minimally coupled to gravity respects positivity bounds applied with the t-channel pole removed. Regardless of whether we consider charged fermions or scalars, we find that it only does so if the effective field theory itself breaks down at the low scale $\Lambda_{\rm new} \sim (emM_{\rm Pl})^{1/2}$, m being the mass of the electron. This result was already anticipated in the renormalizable scalar field theories discussed in [37], and we see that the new features of gauge invariance and spin do not change the essential implications. Furthermore, these results are easily generalized to N_f spinors and N_s scalars

[7]More generally $\gamma(\mu) = \gamma_m - B\ln(\mu/m)$ demonstrating the logarithmic running of the diagrams in Fig. 4.

given that the entire effect comes from one-loop diagrams in which the matter (i.e., electron) is in the loop, and so the relevant amplitude contributions are proportional to N_f and N_s, respectively. Crucially since both scalars and spinors give a characteristically negative contribution to the positivity bound at order $1/M_{\rm Pl}^2$ in graviton exchange, then no choice of N_f and N_s can be used to cancel these contributions and affect these conclusions.

There are three possible perspectives we may take on these results:

(i) *Either* consistent (local) UV completions of QED coupled to gravity do require new physics at scale $\Lambda_{\rm new} \sim (emM_{\rm Pl})^{1/2}$, regardless of whether the UV completion is weakly coupled or strongly coupled;
(ii) *Or* for every charged state, we must impose the unreasonable bounds $m \gtrsim eM_{\rm Pl}/\sqrt{N_*}$, where N_* is the number of fields below the Planck scale, as discussed in Sec. IV D;
(iii) *Or* the positivity bounds do not apply to the t-channel pole subtracted amplitude.

The first conclusion is remarkable in that it is far more stringent than the cutoff expected from the weak gravity conjecture, namely $\Lambda_{\rm WG} \sim eM_{\rm Pl}$ [54], and by extension it is lower than the scale $e^{1/3}M_{\rm Pl}$ [57,58] which is obtained with assumptions on the UV completion from the species bound and Landau pole. Thus if taken seriously, in this context positivity bounds are far more constraining than other "swampland" considerations. The second option while technically valid is a rather unreasonable condition for theories in which the electric charge of all the states is not incredibly small, as in the case of real QED, and so we do not consider it further. The last possibility was discussed in more detail in [37] where we noted there are several reasons to doubt strict positivity in the gravitational context.

A. Absence of decoupling limit

As discussed in [37], the only case in which one can be sure that positivity holds is when there is a clear $M_{\rm Pl} \to \infty$ decoupling limit for which the t-channel pole drops out, provided other terms in the amplitude do not vanish. Interestingly, we can see that this is not possible here without introducing other problems. For instance, for standard QED, $N_f = 1$, in order to take a decoupling limit $M_{\rm Pl} \to \infty$ keeping the scale $\Lambda_{\rm new} \sim (emM_{\rm Pl})^{1/2}$ at least constant for fixed m, or indeed the weak gravity conjecture scale $\Lambda_{\rm WG} = eM_{\rm Pl}$ at least constant, we would need to scale $e \sim 1/M_{\rm Pl}$, meaning we send $M_{\rm Pl} \to \infty$ for fixed $\Lambda_{\rm WG}$ or $\Lambda_{\rm new}$. In doing so the nongravitational part of the amplitude which is of order $e^4/m^4 \sim 1/M_{\rm Pl}^4$ vanishes faster than the $M_{\rm Pl}^2$ suppressed t-channel pole, undermining the very purpose of the decoupling limit since then clearly the graviton exchange dominates. Similarly for the improved amplitude (3.8) the nongravitational part scales as $e^4/\Lambda_{\rm new}^4 \sim 1/M_{\rm Pl}^4$, and we reach the same conclusion.

In many cases a better decoupling limit is obtained by taking $N = N_f + N_s$ species and a large N limit. For instance, one may be tempted to consider a theory with N_f fermions, so that the e^4 suppression of the one-loop amplitude can be compensated by scaling N_f faster than $M_{\rm Pl}^2$. In such a limit $N_f e^4/m^4$ and the one-loop gravitational corrections of the form $N_f e^2/(m^2 M_{\rm Pl}^2)$ dominate over the t-channel pole, suggesting at first sight that an appropriate $M_{\rm Pl} \to \infty$ decoupling limit could be achieved while maintaining some of the relevant physical implications. However, doing so necessarily runs into problems with the species bound [59,60] since then $\Lambda_{\rm species} \sim M_{\rm Pl}/\sqrt{N_f} \to 0$. While not constituting a proof, these arguments are highly suggestive that we should not enforce strict positivity, given the absence of a clean decoupling limit, but rather a weaker condition of the form (1.5), or more precisely in the present context (1.6). We are, of course, free to take the decoupling limit $M_{\rm Pl} \to \infty$ for fixed e and m which in the string amplitude context amounts to $g_s \to 0$ so that the amplitudes are dominated by tree level contributions. However, in this case $\Lambda_{\rm new} \to \infty$ and no contradiction is observed from applying positivity bounds to the tree amplitudes in the nongravitational limit. It is clear that to make further progress it is crucial to establish to what extent positivity bounds apply with gravity, specifically whether it is in the weak sense[8] (1.5) or (1.6), or the stronger one $c > 0$ utilized here.

ACKNOWLEDGMENTS

The work of A. J. T. and C. d. R. is supported by STFC Grants No. ST/P000762/1 and No. ST/T000791/1. C. d. R. thanks the Royal Society for support at ICL through a Wolfson Research Merit Award. L. A. and C. d. R. are supported by the European Union's Horizon 2020 Research Council Grant No. 724659 MassiveCosmo ERC-2016-COG. C. d. R. is also supported by a Simons Foundation Grant No. 555326 under the Simons Foundation's Origins of the Universe initiative, *Cosmology Beyond Einstein's Theory* and by a Simons Investigator Grant No. 690508. S. J. is supported by an STFC studentship. A. J. T. thanks the Royal Society for support at ICL through a Wolfson Research Merit Award.

APPENDIX A: SCALAR QED

1. Conventions

Before jumping into the core of the derivations, it is useful to summarize our relevant conventions. We parametrize the physical momenta of the four particles as

[8] A related discussion is given in the arXiv:v4 version of [42], where the weakening is attributed to a violation of Froissart on the UV. Our perspective is that this assumption is not necessary.

$$k_i^\mu = (k, k\sin\vartheta_i, 0, k\cos\vartheta_i), \tag{A1}$$

with

$$\vartheta_1 = 0, \quad \vartheta_2 = \pi, \quad \vartheta_3 = \theta, \quad \vartheta_4 = \pi + \theta, \tag{A2}$$

where the particles 1,2 are ingoing and 3,4 are outgoing. The quantities k and θ are expressed through the Mandelstam variables using the relations $k^2 = s/4$ and $\cos\theta = 1 + 2t/s$. Similarly, the normalized and transverse polarization vectors are defined as

$$\varepsilon_i^\mu(\pm) = \frac{1}{\sqrt{2}}(0, \cos\vartheta_i, \pm i, -\sin\vartheta_i). \tag{A3}$$

The $2 \to 2$ scattering amplitude in conventions where the momenta are associated with indices as $A^\mu(k_1)$, $A^\nu(k_2)$, $A^\alpha(k_3)$, $A^\beta(k_4)$ reads

$$\mathcal{A}_{\text{physical}}(h_1, h_2, h_3, h_4) = \varepsilon_1^\mu(h_1)\varepsilon_2^\nu(h_2)\mathcal{A}^{\mu\nu\alpha\beta}_{\text{physical}}(k_1, k_2, k_3, k_4)\varepsilon_3^{*\alpha}(h_3)\varepsilon_4^{*\beta}(h_4), \tag{A4}$$

where $h_i = \pm 1$ are the helicities of each particle.

All-ingoing notations.—Henceforth, for computational simplicity we treat also the particles 3,4 as ingoing by reversing their four-momenta: $k_3^\mu = -(k, k\sin\theta, 0, k\cos\theta)$ and $k_4^\mu = -(k, -k\sin\theta, 0, -k\cos\theta)$. We leave the polarization vectors unchanged and calculate the $2 \to 2$ scattering amplitude as

$$\mathcal{A}_{\text{ingoing}}(h_1, h_2, h_3, h_4) = \varepsilon_1^\mu(h_1)\varepsilon_2^\nu(h_2)\mathcal{A}^{\mu\nu\alpha\beta}_{\text{ingoing}}(k_1, k_2, k_3, k_4)\varepsilon_3^{\alpha}(h_3)\varepsilon_4^{\beta}(h_4). \tag{A5}$$

Since under complex conjugation the helicity flips sign, i.e., $\varepsilon_i^{*\mu}(h_i) = \varepsilon_i^\mu(-h_i)$. then an all-ingoing amplitude is mapped to a physical amplitude as $\mathcal{A}_{\text{ingoing}}(h_1, h_2, h_3, h_4) = \mathcal{A}_{\text{physical}}(h_1, h_2, -h_3, -h_4)$. We only use the all-ingoing amplitude (A5) throughout the text and drop the subscript from now on.

We define $(k\varepsilon)_{ij} \equiv k_i \cdot \varepsilon_j$ and $\varepsilon_{ij} \equiv \varepsilon_i \cdot \varepsilon_j$. The inner products between external polarizations in terms of the Mandelstam variables are

$$\begin{aligned}
\varepsilon_{12} &= -\frac{1}{2} - \frac{h_1h_2}{2}, & \varepsilon_{13} &= -\frac{h_1h_3}{2} + \frac{1}{2} + \frac{t}{s},\\
\varepsilon_{14} &= -\frac{h_1h_4}{2} - \frac{1}{2} - \frac{t}{s}, & \varepsilon_{34} &= -\frac{1}{2} - \frac{h_3h_4}{2},\\
\varepsilon_{24} &= -\frac{h_2h_4}{2} + \frac{1}{2} + \frac{t}{s}, & \varepsilon_{23} &= -\frac{h_2h_3}{2} - \frac{1}{2} - \frac{t}{s}.
\end{aligned} \tag{A6}$$

The inner products between external momenta and polarizations are

$$(k\varepsilon)_{13} = (k\varepsilon)_{24} = -\frac{\sqrt{tu}}{\sqrt{2}\sqrt{s}}, \qquad (k\varepsilon)_{14} = (k\varepsilon)_{23} = \frac{\sqrt{tu}}{\sqrt{2}\sqrt{s}}. \tag{A7}$$

These are symmetric $(k\varepsilon)_{ij} = (k\varepsilon)_{ji}$. All other inner products vanish. Note that if all helicities are flipped, all inner products are unchanged since helicity dependence always appears in the form h_ih_j.

2. Tree-level photon-graviton contributions

Irrespective of whether we are interested in the scalar QED Lagrangian (2.2) or the spinor one (2.1), the tree-level photon-graviton contributions are the same. Writing the metric as $g_{\mu\nu} = \eta_{\mu\nu} + h_{\mu\nu}/M_{\text{Pl}}$, the photon-photon-graviton interactions are

$$\mathcal{L}_{hAA} = \frac{1}{2M_{\text{Pl}}}h^{\mu\nu}T_{\mu\nu} = \frac{1}{2M_{\text{Pl}}}h^{\mu\nu}\left(F_{\mu\alpha}F_\nu{}^\alpha - \frac{1}{4}F^{\alpha\beta}F_{\alpha\beta}\eta_{\mu\nu}\right), \tag{A8}$$

where all indices are raised/lowered with the Minkowski metric $\eta_{\mu\nu}$. The Feynman rule for the $h^{\alpha\beta}A^\mu(k_1)A^\nu(k_2)$ vertex is then

$$\begin{aligned}
\mathcal{V}^{\mu\nu;\alpha\beta} \equiv{}& \frac{i}{2}k_1\cdot k_2(\eta^{\alpha\beta}\eta^{\mu\nu} - 2\eta^{\nu(\beta}\eta^{\alpha)\mu}) - \frac{i}{2}\eta^{\alpha\beta}k_1^\nu k_2^\mu\\
&- i\eta^{\mu\nu}k_1^{(\alpha}k_2^{\beta)} + i(k_2^\mu\eta^{\nu(\alpha}k_1^{\beta)} + k_2^{(\beta}\eta^{\alpha)\mu}k_1^\nu).
\end{aligned} \tag{A9}$$

The d-dimensional graviton propagator is (in harmonic/de Donder gauge)

$$D_{\alpha\beta;\gamma\delta}(k^2) = -\frac{2i}{k^2}\left(\eta_{\alpha\delta}\eta_{\beta\gamma} + \eta_{\alpha\gamma}\eta_{\beta\delta} - \frac{2\eta_{\alpha\beta}\eta_{\gamma\delta}}{d-2}\right). \tag{A10}$$

At tree level we are free to set $d = 4$. Then the s-diagram gives

$$M_{\rm Pl}^2\mathcal{A}_s = -i\varepsilon_{1\chi}\varepsilon_{2\kappa}\mathcal{V}^{\chi\kappa;\alpha\beta}D_{\alpha\beta;\gamma\delta}(-s)\mathcal{V}^{\mu\nu,\gamma\delta}\varepsilon_{3\mu}\varepsilon_{4\nu}$$
$$= \varepsilon_{12}\varepsilon_{34}\left(s-\frac{t^2}{2s}-\frac{u^2}{2s}\right)-\frac{1}{2}(\varepsilon_{14}\varepsilon_{23}+\varepsilon_{13}\varepsilon_{24})s+\frac{tu}{s}(\varepsilon_{12}+\varepsilon_{34})$$
$$= \frac{-1}{8s}(t^2(h_1(h_2h_3h_4-h_2+h_3-h_4)-h_2(h_3-h_4)-h_3h_4+1)$$
$$+u^2(h_1(h_2h_3h_4-h_2-h_3+h_4)-h_4(h_2+h_3)+h_2h_3+1)). \tag{A11}$$

The t-diagram gives

$$M_{\rm Pl}^2\mathcal{A}_t = -i\varepsilon_{1\chi}\varepsilon_{3\kappa}\mathcal{V}^{\chi\kappa;\alpha\beta}D_{\alpha\beta;\gamma\delta}(-t)\mathcal{V}^{\mu\nu,\gamma\delta}\varepsilon_{2\mu}\varepsilon_{4\nu}$$
$$= \frac{-1}{8t}(u^2(h_1(h_2h_3h_4-h_2-h_3+h_4)-h_4(h_2+h_3)+h_2h_3+1)$$
$$+s^2(h_1(h_2h_3h_4+h_2-h_3-h_4)-h_2(h_3+h_4)+h_3h_4+1)), \tag{A12}$$

and the u-diagram gives

$$M_{\rm Pl}^2\mathcal{A}_u = -i\varepsilon_{1\chi}\varepsilon_{4\kappa}\mathcal{V}^{\chi\kappa;\alpha\beta}D_{\alpha\beta;\gamma\delta}(-u)\mathcal{V}^{\mu\nu,\gamma\delta}\varepsilon_{2\mu}\varepsilon_{3\nu}$$
$$= \frac{-1}{8u}(t^2(h_1(h_2h_3h_4-h_2+h_3-h_4)+h_2(h_4-h_3)-h_3h_4+1)$$
$$+s^2(h_1(h_2h_3h_4+h_2-h_3-h_4)-h_2(h_3+h_4)+h_3h_4+1)). \tag{A13}$$

Combining those three channels together we have

$$\mathcal{A}_{\text{tree},0}(h_1,h_2,h_3,h_4) = \frac{-1}{4M_{\rm Pl}^2stu}\Big[(-1+h_1h_2)(-1+h_3h_4)(t^4+u^4-\frac{1}{4}(s^2+t^2+u^2)^2)$$
$$+(-1+h_1h_3)(-1+h_2h_4)(s^4+u^4-\frac{1}{4}(s^2+t^2+u^2)^2)$$
$$-(-1+h_2h_3)(-1+h_1h_4)(u^4-\frac{1}{4}(s^2+t^2+u^2)^2)\Big], \tag{A14}$$

which give the familiar results for example processes

$$\mathcal{A}(++++)=0=\mathcal{A}(+++-),$$
$$\mathcal{A}(++--)=\frac{1}{M_{\rm Pl}^2}\frac{s^4}{stu},$$
$$\mathcal{A}(+-+-)=\frac{1}{M_{\rm Pl}^2}\frac{t^4}{stu},$$
$$\mathcal{A}(+--+)=\frac{1}{M_{\rm Pl}^2}\frac{u^4}{stu}. \tag{A15}$$

3. Photon wave function renormalization

At one-loop there are two diagrams contributing to the quantum photon propagator given in Fig. 5. The self-energy of the photon $\Pi^{\rho\sigma}(k^2)$ obeys the Ward identity $k_\rho\Pi^{\rho\sigma}(k^2)=0$ implying that the self-energy is proportional to the projector onto the subspace transverse to k^μ,

$$\Pi^{\rho\sigma}(k^2) = (k^2\eta^{\rho\sigma}-k^\rho k^\sigma)\Pi(k^2). \tag{A16}$$

The two diagrams give

(a) Specific to scalar QED. (b) For both scalar and spinor QED.

FIG. 5. One-loop self-energy contribution for scalar and spinor QED.

$$\begin{aligned}\Pi^{\rho\sigma}(k^2) &= e^2\mu^\epsilon \int \frac{\mathrm{d}^d p}{(2\pi)^d}\frac{(2p-k)^\rho(2p-k)^\sigma}{(p^2+m^2)((p-k)^2+m^2)} - 2e^2\eta^{\rho\sigma}\int\frac{\mathrm{d}^d p}{(2\pi)^d}\frac{1}{p^2+m^2}\\ &= e^2\mu^\epsilon\int\frac{\mathrm{d}^d p}{(2\pi)^d}\frac{(2p-k)^\rho(2p-k)^\sigma - 2\eta^{\rho\sigma}((p-k)^2+m^2)}{(p^2+m^2)((p-k)^2+m^2)}\\ &= e^2\mu^\epsilon\int\frac{\mathrm{d}^d l}{(2\pi)^d}\int_0^1 \mathrm{d}x\frac{(\frac{4}{d}-2)\eta^{\rho\sigma}l^2 - 2\eta^{\rho\sigma}(k^2+m^2+k^2x^2-2k^2x)+k^\rho k^\sigma(1-4x+4x^2)}{(l^2+m^2+xk^2(1-x))^2}\\ &= -\frac{ie^2}{4\pi^2}\int_{-\frac{1}{2}}^{\frac{1}{2}}\mathrm{d}y y^2(k^2\eta^{\rho\sigma}-k^\rho k^\sigma)\ln\frac{\mu^2}{m^2-k^2(y^2-\frac{1}{4})},\end{aligned} \tag{A17}$$

where in the last step the Feynman parameter is redefined by $y = x - \frac{1}{2}$. By resumming the series of one-particle irreducible (1PI) diagrams contributing to the quantum propagator, one can show that the wave function renormalization is

$$Z_A = \frac{1}{1+i\Pi(0)}. \tag{A18}$$

The scalar part of the self-energy can be found from the expression above to be

$$\Pi(k^2) = -\frac{ie^2}{4\pi^2}\int_{-\frac{1}{2}}^{\frac{1}{2}}\mathrm{d}y y^2\ln\frac{\mu^2}{m^2-k^2(y^2-\frac{1}{4})}, \tag{A19}$$

so that

$$\Pi(0) = -\frac{ie^2}{48\pi^2}\ln\frac{\mu^2}{m^2}, \tag{A20}$$

and thus

$$Z_A = 1 - \frac{e^2}{48\pi^2}\ln\frac{\mu^2}{m^2} + \mathcal{O}(e^4). \tag{A21}$$

4. Nongravitational contributions

By nongravitational contributions, we refer to the Feynman diagrams with no graviton lines, shown in the first line of Fig. 2. There are no nongravitational tree diagrams so we start at one-loop. From diagrams with two internal propagators we get three crossing related diagrams giving the familiar expressions

$$\begin{aligned}\mathcal{A}_{2-s} &= \frac{e^4}{4\pi^2}(\varepsilon_1\cdot\varepsilon_2)(\varepsilon_3\cdot\varepsilon_4)\int_0^1\mathrm{d}x\left(\overline{\mathrm{MS}}+\ln\frac{\mu^2}{m^2+sx(x-1)}\right),\\ \mathcal{A}_{2-t} &= \frac{e^4}{4\pi^2}(\varepsilon_1\cdot\varepsilon_3)(\varepsilon_2\cdot\varepsilon_4)\int_0^1\mathrm{d}x\left(\overline{\mathrm{MS}}+\ln\frac{\mu^2}{m^2+tx(x-1)}\right),\\ \mathcal{A}_{2-u} &= \frac{e^4}{4\pi^2}(\varepsilon_1\cdot\varepsilon_4)(\varepsilon_2\cdot\varepsilon_3)\int_0^1\mathrm{d}x\left(\overline{\mathrm{MS}}+\ln\frac{\mu^2}{m^2+ux(x-1)}\right).\end{aligned} \tag{A22}$$

Next we have diagrams that have three internal ϕ propagators in the loop which give (including a factor of 2 for charge flow reversal)

$$\begin{aligned}\mathcal{A}_{3-s} &= i32e^4\mu^\epsilon\int\frac{\mathrm{d}^d l}{(2\pi)^d}\mathrm{d}x\mathrm{d}y\frac{\frac{2}{d}l^2\varepsilon_{12}\varepsilon_{34}-(k\varepsilon)_{12}(k\varepsilon)_{21}\varepsilon_{34}xy-(k\varepsilon)_{34}(k\varepsilon)_{43}\varepsilon_{12}xy}{(l^2+m^2-sxy)^3}\\ &= -\frac{e^4}{\pi^2}\int\mathrm{d}x\mathrm{d}y\left(\varepsilon_{12}\varepsilon_{34}\ln\frac{\mu^2}{m^2-sxy}-\frac{xy((k\varepsilon)_{12}(k\varepsilon)_{21}\varepsilon_{34}+(k\varepsilon)_{34}(k\varepsilon)_{43}\varepsilon_{12})}{(m^2-sxy)}\right)\\ &= -\frac{e^4}{\pi^2}\int\mathrm{d}x\mathrm{d}y\left(\varepsilon_{12}\varepsilon_{34}\ln\frac{\mu^2}{m^2-sxy}\right).\end{aligned} \tag{A23}$$

The other channels are given by

$$\begin{aligned}\mathcal{A}_{3-t} &= -\frac{e^4}{\pi^2}\int\mathrm{d}x\mathrm{d}y\left(\varepsilon_{13}\varepsilon_{24}\ln\frac{\mu^2}{m^2-txy}-\frac{xytu(\varepsilon_{24}+\varepsilon_{13})}{2s(m^2-txy)}\right),\\ \mathcal{A}_{3-u} &= -\frac{e^4}{\pi^2}\int\mathrm{d}x\mathrm{d}y\left(\varepsilon_{14}\varepsilon_{23}\ln\frac{\mu^2}{m^2-uxy}-\frac{xytu(\varepsilon_{23}+\varepsilon_{14})}{2s(m^2-uxy)}\right).\end{aligned} \tag{A24}$$

Finally there are three diagrams (in addition to their charge reversal) with four internal ϕ propagators, i.e., the box diagram, as the last diagram on the first line of Fig. 2,

$$i\mathcal{A}_{4-s} = 16e^4\mu^\epsilon \int \frac{\mathrm{d}^d p}{(2\pi)^d} \frac{(p\varepsilon_1)(p\varepsilon_3)(p\varepsilon_4 + (k\varepsilon)_{34})(p\varepsilon_2 - (k\varepsilon)_{12})}{(p^2+m^2)((p+k_3)^2+m^2)((p-k_1)^2+m^2)((p+(k_3+k_4))^2+m^2)}. \tag{A25}$$

Shifting the loop momentum, $l = p + xk_3 - yk_1 + z(k_3+k_4)$ and including the factors of 2 from charge reversal,

$$i\mathcal{A}_{4-s} = 2\times 3!\times 16e^4\mu^\epsilon \int \frac{\mathrm{d}^d l}{(2\pi)^d}\mathrm{d}x\mathrm{d}y\mathrm{d}z \frac{Al^4 + Bl^2 + C}{(l^2+m^2+sz(x+z+y-1)-tyx)^4}, \tag{A26}$$

where

$$\begin{aligned} A &= \frac{\varepsilon_{12}\varepsilon_{34} + \varepsilon_{13}\varepsilon_{24} + \varepsilon_{14}\varepsilon_{23}}{d(d+2)}, \\ B &= \frac{-tu(\varepsilon_{34}x^2 + (\varepsilon_{13} - \varepsilon_{23} - \varepsilon_{14} + \varepsilon_{24})xy + \varepsilon_{12}y^2)}{2ds}, \\ C &= \frac{t^2u^2x^2y^2}{4s^2}. \end{aligned} \tag{A27}$$

The other diagrams are computed similarly,

$$i\mathcal{A}_{4-u} = 2\times 3!\times 16e^4\mu^\epsilon \int \frac{\mathrm{d}^d l}{(2\pi)^d}\mathrm{d}x\mathrm{d}y\mathrm{d}z \frac{Al^4 + Dl^2 + E}{(l^2+m^2+uz(x+z+y-1)-tyx)^4}, \tag{A28}$$

where

$$\begin{aligned} D &= \frac{tu}{2ds^2} f(\{h_i\}, s, t), \\ E &= \frac{t^2u^2(x+z-1)(x+z)(y+z-1)(y+z)}{4s^2}, \end{aligned} \tag{A29}$$

where f is linear in s and t (with no terms such as st). Finally the t-channel contribution gives

$$i\mathcal{A}_{4-t} = 2\times 3!\times 16e^4\mu^\epsilon \int \frac{\mathrm{d}^d l}{(2\pi)^d}\mathrm{d}x\mathrm{d}y\mathrm{d}z \frac{Al^4 + Fl^2 + C}{(l^2+m^2+sz(x+z+y-1)-uyx)^4}, \tag{A30}$$

where

$$F = \frac{-tu(\varepsilon_{34}x^2 - (\varepsilon_{13} - \varepsilon_{23} - \varepsilon_{14} + \varepsilon_{24})xy + \varepsilon_{12}y^2)}{2ds}. \tag{A31}$$

The full expression for D is

$$\begin{aligned} D = {} & \frac{h_1h_2tuyz}{2ds} + \frac{h_1h_2tuy^2}{4ds} - \frac{h_1h_2tuy}{4ds} + \frac{h_1h_2tuz^2}{4ds} - \frac{h_1h_2tuz}{4ds} + \frac{h_1h_3tuxy}{4ds} + \frac{h_1h_3tuxz}{4ds} - \frac{h_1h_3tux}{4ds} + \frac{h_1h_3tuyz}{4ds} - \frac{h_1h_3tuy}{4ds} \\ & + \frac{h_1h_3tuz^2}{4ds} - \frac{h_1h_3tuz}{2ds} + \frac{h_1h_3tu}{4ds} - \frac{h_1h_4tuxy}{4ds} - \frac{h_1h_4tuxz}{4ds} - \frac{h_1h_4tuyz}{4ds} + \frac{h_1h_4tuy}{4ds} + \frac{h_1h_4tuz}{4ds} - \frac{h_1h_4tuz^2}{4ds} \\ & - \frac{h_2h_3tuxy}{4ds} - \frac{h_2h_3tuxz}{4ds} + \frac{h_2h_3tux}{4ds} - \frac{h_2h_3tuyz}{4ds} + \frac{h_2h_3tuz}{4ds} - \frac{h_2h_3tuz^2}{4ds} + \frac{h_2h_4tuxy}{4ds} + \frac{h_2h_4tuxz}{4ds} + \frac{h_2h_4tuyz}{4ds} \\ & + \frac{h_2h_4tuz^2}{4ds} + \frac{h_3h_4tuxz}{2ds} + \frac{h_3h_4tux^2}{4ds} - \frac{h_3h_4tux}{4ds} + \frac{h_3h_4tuz^2}{4ds} - \frac{h_3h_4tuz}{4ds} - \frac{2t^2uxy}{ds^2} - \frac{tuxy}{ds} - \frac{2t^2uxz}{ds^2} - \frac{tuxz}{2ds} + \frac{t^2ux}{ds^2} \\ & + \frac{tux^2}{4ds} + \frac{tux}{4ds} - \frac{2t^2uyz}{ds^2} - \frac{tuyz}{2ds} + \frac{t^2uy}{ds^2} + \frac{tuy^2}{4ds} + \frac{tuy}{4ds} + \frac{2t^2uz}{ds^2} - \frac{2t^2uz^2}{ds^2} + \frac{tuz}{2ds} - \frac{tuz^2}{2ds} - \frac{t^2u}{2ds^2} - \frac{tu}{4ds}. \end{aligned} \tag{A32}$$

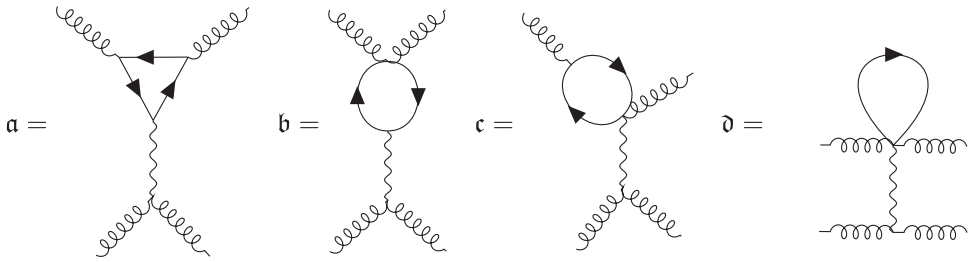

FIG. 6. Four classes of gravitational diagrams contributing at one-loop and to order $1/M_{\rm Pl}^2$. The arrows depict the direction of the charge flow. We do not show all the crossed versions of the diagrams.

RG scale independence of nongravitational contributions.—A consistency check of numerical factors is to see that all dependence on the scale μ drops out of the total amplitude. The two-propagator loop diagrams give the μ dependent term,

$$\frac{e^4}{4\pi^2}(\varepsilon_{12}\varepsilon_{34}+\varepsilon_{13}\varepsilon_{24}+\varepsilon_{14}\varepsilon_{23})\ln\frac{\mu^2}{m^2}, \tag{A33}$$

from the three-propagator diagrams we have

$$-\frac{1}{2}\times\frac{e^4}{\pi^2}(\varepsilon_{12}\varepsilon_{34}+\varepsilon_{13}\varepsilon_{24}+\varepsilon_{14}\varepsilon_{23})\ln\frac{\mu^2}{m^2}, \tag{A34}$$

and from the four-propagator diagrams we have

$$3\times 2\times 3!\times 16\times\frac{1}{6}\times\frac{1}{384\pi^2}(\varepsilon_{12}\varepsilon_{34}+\varepsilon_{13}\varepsilon_{24}+\varepsilon_{14}\varepsilon_{23})\ln\frac{\mu^2}{m^2}. \tag{A35}$$

Summing these terms gives zero so there is no μ dependence.

5. One-loop graviton exchange

The diagrams relevant for the one-loop graviton exchange are given in Fig. 6. It is understood that each type of diagrams should also include flipped versions, with loops on the other end of the graviton line or on different photon lines as well as the crossed versions of each diagram. We now proceed with deriving the contributions to the discontinuity from each of these types of diagrams.

a. Type 𝔞 diagrams

Summing the diagrams of type 𝔞 and their flipped version we obtain for the t-channel amplitude

$$i\mathcal{A}_{\mathfrak{a}-t}=(-i)^5\times 2!\times 2\times 4e^2\int\frac{\mathrm{d}^d l}{(2\pi)^d}\mathrm{d}x\mathrm{d}y\frac{Al^4+Bl^2+C}{(l^2+m^2-xyt)^3}. \tag{A36}$$

The factor of 2! is due to combining propagators, the factor of 2 is due to doubling of the term by a loop charge direction reversal, and the factor of 4 just comes from the two QED-like vertices. If we call the $(+,+,-,-)$, $(+,-,-,+)$, $(+,-,+,-)$ configurations I, II, III, respectively, then the numerator coefficients are

$$\begin{aligned}
A_{\rm I}&=\frac{2i(2(d-2)st+dsu+(d-4)s^2+(d-4)t(t+u))}{d(d+2)s^2}=-\frac{8i}{d(d+2)}=-\frac{i}{3}-\frac{5i\epsilon}{36}+\mathcal{O}(\epsilon^2),\\
A_{\rm II}&=\frac{2i(d-4)(s+t)(s+t+u)}{d(d+2)s^2}=0,\\
A_{\rm III}&=\frac{2i(d-4)t(t+u)}{d(d+2)s^2}=-\frac{2i(d-4)t}{d(d+2)s}=\frac{it\epsilon}{12s}+\mathcal{O}(\epsilon^2),\\
B_{\rm I}&=-\frac{2i(s+t)(x+y-1)(s(x+y-1)+3t(x+y)-t)}{dt},\\
B_{\rm II}&=-\frac{2i(s+t)^2(x+y-1)^2}{dt},\\
B_{\rm III}&=-\frac{i(d-4)t((d-2)xy(s+t)+2m^2)}{(d-2)ds}=\frac{it\epsilon(m^2+sxy+txy)}{4s}+\mathcal{O}(\epsilon^2),\\
C_{\rm I}&=-ixyu^2(x+y-1)^2,\qquad C_{\rm II}=-ixyu^2(x+y-1)^2,\qquad C_{\rm III}=\frac{i(d-4)m^2txyu}{(d-2)s}=\mathcal{O}(\epsilon).
\end{aligned} \tag{A37}$$

Note that for the C coefficients, if they are of order ϵ they can be set to zero as the dim-reg integrals do not produce $1/\epsilon$ terms that would combine with them to make them finite. Moving on to the s-channel of diagram $\mathfrak{a}$ we have

$$i\mathcal{A}_{\mathfrak{a}-s} = (-i)^5 \times 2! \times 2 \times 4e^2 \int \frac{\mathrm{d}^d l}{(2\pi)^d} \mathrm{d}x\mathrm{d}y \frac{Dl^4 + El^2 + F}{(l^2 + m^2 - xys)^3}, \tag{A38}$$

$$\begin{aligned} D_{\mathrm{I}} &= \frac{2i(d-4)}{d(d+2)} = -\frac{i\epsilon}{12} + \mathcal{O}(\epsilon^2), \\ D_{\mathrm{II}} &= -\frac{8iu^2}{d(d+2)s^2} = -\frac{5iu^2\epsilon}{36s^2} - \frac{iu^2}{3s^2}, \\ D_{\mathrm{III}} &= -\frac{8it^2}{d(d+2)s^2} = -\frac{5it^2\epsilon}{36s^2} - \frac{it^2}{3s^2}, \\ E_{\mathrm{I}} &= \frac{2i(d-4)m^2}{(d-2)d} = -\frac{im^2\epsilon}{4}, \qquad E_{\mathrm{II}} = 0, \\ E_{\mathrm{III}} &= 0, \qquad F_{\mathrm{I}} = 0, \qquad F_{\mathrm{II}} = 0, \qquad F_{\mathrm{III}} = 0. \end{aligned} \tag{A39}$$

Finally, the u-channel gives

$$i\mathcal{A}_{\mathfrak{a}-u} = (-i)^5 \times 2! \times 2 \times 4e^2 \int \frac{\mathrm{d}^d l}{(2\pi)^d} \mathrm{d}x\mathrm{d}y \frac{Gl^4 + Hl^2 + I}{(l^2 + m^2 - xyu)^3}, \tag{A40}$$

with

$$\begin{aligned} G_{\mathrm{I}} &= -\frac{8i}{d(d+2)} = -\frac{5i\epsilon}{36} - \frac{i}{3} + \mathcal{O}(\epsilon^2), \\ G_{\mathrm{II}} &= -\frac{2i(d-4)u}{d(d+2)s} = \frac{i\epsilon u}{12s}, \qquad G_{\mathrm{III}} = 0, \\ H_{\mathrm{I}} &= -\frac{2it(x+y-1)(2s(x+y)+t(-1+3x+3y))}{du}, \\ H_{\mathrm{II}} &= \frac{i(d-4)u((d-2)txy-2m^2)}{(d-2)ds}, \\ H_{\mathrm{III}} &= -\frac{2it^2(x+y-1)^2}{du}, \\ I_{\mathrm{I}} &= -it^2xy(x+y-1)^2, \\ I_{\mathrm{II}} &= \frac{i(d-4)m^2tuxy}{(d-2)s}, \\ I_{\mathrm{III}} &= -it^2xy(x+y-1)^2. \end{aligned} \tag{A41}$$

b. Type $\mathfrak{b}$ diagrams

For type $\mathfrak{b}$ diagrams (including their version flipped up-down) we find the general expression

$$i\mathcal{A}_{\mathfrak{b}-t} = (-i)^3 \times 2e^2 \int \frac{\mathrm{d}^d l}{(2\pi)^d} \mathrm{d}x \frac{Jl^2 + K}{(l^2 + m^2 - x(1-x)t)^2}, \tag{A42}$$

$$\begin{aligned} J_{\mathrm{I}} &= J_{\mathrm{II}} = 0, \qquad J_{\mathrm{III}} = \frac{2i(d-4)t(t+u)}{ds^2}, \\ K_{\mathrm{I}} &= K_{\mathrm{II}} = 0, \qquad K_{\mathrm{III}} = -\frac{2i(d-4)m^2t}{(d-2)s}. \end{aligned} \tag{A43}$$

The s-channel has the expressions

$$i\mathcal{A}_{\mathfrak{b}-s} = (-i)^3 \times 2e^2 \int \frac{\mathrm{d}^d l}{(2\pi)^d} \mathrm{d}x \frac{Ll^2 + M}{(l^2 + m^2 - x(1-x)s)^2}, \tag{A44}$$

$$\begin{aligned} L_{\mathrm{I}} &= \frac{2i(d-4)}{d}, \qquad L_{\mathrm{II}} = 0, \qquad L_{\mathrm{III}} = 0, \\ M_{\mathrm{I}} &= \frac{2i(d-4)m^2}{d-2}, \qquad M_{\mathrm{II}} = 0, \qquad M_{\mathrm{III}} = 0, \end{aligned} \tag{A45}$$

while the u-channel leads to

$$i\mathcal{A}_{\mathfrak{b}-u} = (-i)^3 \times 2e^2 \int \frac{\mathrm{d}^d l}{(2\pi)^d} \mathrm{d}x \frac{Nl^2 + O}{(l^2 + m^2 - x(1-x)u)^2}, \tag{A46}$$

$$\begin{aligned} N_{\mathrm{I}} &= 0, \quad N_{\mathrm{II}} = \frac{-2i(d-4)u}{ds}, \quad N_{\mathrm{III}} = 0, \\ O_{\mathrm{I}} &= 0, \quad O_{\mathrm{II}} = \frac{-2i(d-4)m^2u}{(d-2)s}, \quad O_{\mathrm{III}} = 0. \end{aligned} \tag{A47}$$

c. Type $\mathfrak{c}$ diagrams

This type of diagrams relies on the quartic $\phi\phi^\dagger h_{\alpha\beta}A_\gamma$ interactions that arise from the following terms in the action:

$$\begin{aligned} & ie\sqrt{-g}g^{\mu\nu}A_\mu(\phi\partial_\nu\phi^\dagger - \partial_\nu\phi\phi^\dagger) \\ & \supset -iehh^{\mu\nu}A_\mu(\phi\partial_\nu\phi^\dagger - \partial_\nu\phi\phi^\dagger) \\ & \quad + \frac{1}{2}iehA^\nu(\phi\partial_\nu\phi^\dagger - \partial_\nu\phi\phi^\dagger). \end{aligned} \tag{A48}$$

This leads to the rule (momenta ingoing)

$$\mathcal{V}_{\phi\phi^\dagger hA} = -ie\eta_{\gamma(\alpha}(k_1 - k_2)_{\beta)} + \frac{i}{2}e\eta_{\alpha\beta}(k_1 - k_2)_\gamma. \tag{A49}$$

Summing the diagrams gives

$$i\mathcal{A}_{\mathfrak{c}} = 2i^3e^2 \int \frac{\mathrm{d}^d l}{(2\pi)^d} \frac{Pl^2}{(l^2 + m^2)^2}, \tag{A50}$$

$$P_{\rm I} = \frac{16i}{d} + 0 + \frac{16i}{d}, \qquad P_{\rm II} = 0 + \frac{16iu^2}{ds^2} + 0,$$
$$P_{\rm III} = 0 + \frac{16it^2}{ds^2} + 0. \tag{A51}$$

Since the denominator of the loop integral is the same for all channels, we may simply sum them up and each term in the previous $P_{\rm I,II,III}$ sums denotes the t, s, u-channel contributions, respectively.

d. Type $\mathfrak{d}$ diagrams

There is a new interaction vertex $\phi\phi^\dagger h_{\alpha\beta}A_\gamma A_\delta$ from the terms

$$-\sqrt{-g}g^{\mu\nu}e^2A_\mu A_\nu\phi\phi^\dagger \supset -\frac{h}{2}\eta^{\mu\nu}e^2A_\mu A_\nu + h^{\mu\nu}e^2A_\mu A_\nu, \tag{A52}$$

with rule

$$\mathcal{V}_{\phi\phi^\dagger hAA} = ie^2(-\eta_{\alpha\beta}\eta_{\gamma\delta} + 2\eta_{\alpha(\gamma}\eta_{\delta)\beta}). \tag{A53}$$

Summing the diagrams gives

$$i\mathcal{A}_{\mathfrak{d}} = -ie^2\int\frac{{\rm d}^dl}{(2\pi)^d}\frac{Q}{(l^2+m^2)}, \tag{A54}$$

$$Q_{\rm I} = -8i + 0 - 8i, \qquad Q_{\rm II} = 0 - \frac{8iu^2}{s^2} + 0,$$
$$Q_{\rm III} = 0 - \frac{8it^2}{s^2} + 0. \tag{A55}$$

Again the terms denote the t, s, u-channel contributions, respectively.

6. Consistency checks

a. Pole cancellations

The previous derivations present poles for various types of diagrams at $s=0$ and $t=0$ (for configuration II) and at $u=0$ (for configuration III). In what follows we shall see that these pole contributions precisely cancel out when accounting for the wave function renormalization.

1. Pole cancellation for configuration II

The sum of all $\mathfrak{a},\mathfrak{b},\mathfrak{c},\mathfrak{d}$ diagrams for configuration II contains a pole at $s=0$ and at $t=0$ and no pole at $u=0$. The $t=0$ pole is

$$M_{\rm Pl}^2\mathcal{A}_{\rm II}^{\text{1-loop}} \supset -\frac{e^2}{2\pi^2}\frac{u^2}{t}\int{\rm d}x{\rm d}y(x+y-1)^2\ln\frac{\mu^2}{m^2} = -\frac{e^2}{24\pi^2}\frac{u^2}{t}\ln\frac{\mu^2}{m^2}, \tag{A56}$$

directly canceling the correction from wave function renormalization. The $s=0$ pole arises in the s-channel diagram giving the coefficient $D_{\rm II}$ and is

$$M_{\rm Pl}^2\mathcal{A}_{\rm II}^{\text{1-loop}} \supset -\frac{e^2}{\pi^2}\frac{u^2}{s}\int{\rm d}x{\rm d}yxy\ln\frac{\mu^2}{m^2} = -\frac{e^2}{24\pi^2}\frac{u^2}{s}\ln\frac{\mu^2}{m^2}, \tag{A57}$$

canceling the wave function renormalization piece.

2. Pole cancellation for configuration III

The sum of all $\mathfrak{a},\mathfrak{b},\mathfrak{c},\mathfrak{d}$ diagrams for configuration III contains a pole at $u=0$,

$$M_{\rm Pl}^2\mathcal{A}_{\rm III}^{\text{1-loop}} \supset -\frac{e^2}{2\pi^2}\frac{t^2}{u}\int{\rm d}x{\rm d}y(x+y-1)^2\ln\frac{\mu^2}{m^2} = -\frac{e^2}{24\pi^2}\frac{t^2}{u}\ln\frac{\mu^2}{m^2}, \tag{A58}$$

canceling the wave function renormalization piece. The $s=0$ pole arises in the s-channel diagram giving the coefficient $D_{\rm III}$ and is

$$M_{\rm Pl}^2\mathcal{A}_{\rm III}^{\text{1-loop}} \supset -\frac{e^2}{\pi^2}\frac{t^2}{s}\int{\rm d}x{\rm d}yxy\ln\frac{\mu^2}{m^2} = -\frac{e^2}{24\pi^2}\frac{u^2}{s}\ln\frac{\mu^2}{m^2}, \tag{A59}$$

canceling the wave function renormalization piece.

b. RG scale independence

Again as a sanity check, we can verify that all dependence on the renormalization scale μ drops out of the total amplitude from this gravitational exchange. We can check this explicitly for the various configurations.

1. Configuration I

Considering the type $\mathfrak{a}$ diagrams we get the μ dependence,

$$M_{\rm Pl}^2\mathcal{A}_{\rm I} \supset \frac{s^3+24m^2tu}{24\pi^2tu}e^2\ln\frac{\mu^2}{m^2} = \left(\frac{1}{24\pi^2}\frac{s^4}{stu} + \frac{m^2}{\pi^2}\right)e^2\ln\frac{\mu^2}{m^2}. \tag{A60}$$

The first term here cancels against the wave function renormalization correction to the tree amplitude. The type $\mathfrak{b}$ diagrams do not give any μ dependent terms as all loop integrands are proportional to $d-4$. The remaining diagrams give an RG dependence,

$$M_{\rm Pl}^2\mathcal{A}_{\rm I} \supset -e^2\frac{m^2}{\pi^2}\ln\frac{\mu^2}{m^2}, \tag{A61}$$

so the total μ dependence cancels.

2. Configuration II

Considering the type $\mathfrak{a}$ diagrams we get the μ dependence,

$$M_{\rm Pl}^2\mathcal{A}_{\rm II} \supset \frac{su^3+12m^2tu^2}{24\pi^2s^2t}e^2\ln\frac{\mu^2}{m^2} = \left(\frac{1}{24\pi^2}\frac{u^4}{stu}+\frac{m^2u^2}{2\pi^2s^2}\right)e^2\ln\frac{\mu^2}{m^2}. \tag{A62}$$

The first term here cancels against the wave function renormalization correction to the tree amplitude. The type $\mathfrak{b}$ diagrams do not give any μ dependent terms as all loop integrands are proportional to $d-4$. The remaining diagrams give an RG dependence,

$$M_{\rm Pl}^2\mathcal{A}_{\rm II} \supset -e^2\frac{m^2u^2}{2\pi^2s^2}\ln\frac{\mu^2}{m^2}, \tag{A63}$$

so the total μ dependence cancels.

3. Configuration III

Considering the type $\mathfrak{a}$ diagrams we get the μ dependence,

$$M_{\rm Pl}^2\mathcal{A}_{\rm III} \supset \frac{st^3+12m^2ut^2}{24\pi^2s^2u}e^2\ln\frac{\mu^2}{m^2} = \left(\frac{1}{24\pi^2}\frac{t^4}{stu}+\frac{m^2t^2}{2\pi^2s^2}\right)e^2\ln\frac{\mu^2}{m^2}. \tag{A64}$$

The first term here cancels against the wave function renormalization correction to the tree amplitude. The type $\mathfrak{b}$ diagrams do not give any μ dependent terms as all loop integrands are proportional to $d-4$. The remaining diagrams give an RG dependence,

$$M_{\rm Pl}^2\mathcal{A}_{\rm III} \supset -e^2\frac{m^2t^2}{2\pi^2s^2}\ln\frac{\mu^2}{m^2}, \tag{A65}$$

so again the total μ dependence cancels.

APPENDIX B: SPINOR QED

We now turn to the analogous derivation for spinor QED. We refer to Appendix A 1 for a summary of our conventions. As mentioned in Appendix A 2, the tree-level photon-graviton contributions are exactly the same for scalar and spinor QED, and we therefore refer to that Appendix for those tree-level contributions. In what follows we can simply focus on deriving the one-loop diagrams that arise in spinor QED.

1. Curved spacetime action

The action for spinor electrodynamics in flat space is

$$S = \int \mathrm{d}^4x\left(-\frac{1}{4}F^{\mu\nu}F_{\mu\nu}+\bar\psi(i\not{D}-m)\psi\right), \tag{B1}$$

where $\not{D}=\gamma^\mu(\partial_\mu - ieA_\mu)$. The electron is a Dirac spinor denoted ψ and the Dirac adjoint is $\bar\psi\equiv\psi^\dagger\gamma^0$ (suppressing spinor indices). The propagator for a fermion is

$$S_F = \frac{-i(-\not{p}+m)}{p^2+m^2-i\epsilon}. \tag{B2}$$

To minimally couple this to gravity we use a vierbein to set up local inertial frames in which the gamma matrices take their usual constant form,

$$S = \int \mathrm{d}^4x\sqrt{-g}\left(-\frac{1}{4}F^{\mu\nu}F_{\mu\nu} + \bar\psi\gamma^A v_A^\mu(i\nabla_\mu+eA_\mu)\psi - m\bar\psi\psi\right), \tag{B3}$$

where $\nabla_\mu=\partial_\mu-\frac{1}{2}\omega_{\mu AB}J^{AB}$, with $J^{AB}=\frac{1}{4}[\gamma^A,\gamma^B]$, and $\omega_{\mu AB}$ is the spin connection. Here the inverse vierbein is denoted v_A^μ. The gamma matrices satisfy

$$\{\gamma^\mu,\gamma^\nu\}=-2g^{\mu\nu}, \qquad \{\gamma^A,\gamma^B\}=-2\eta^{AB}. \tag{B4}$$

We can write the metric as a perturbation around Minkowski space, $g_{\mu\nu}=\eta_{\mu\nu}+\kappa h_{\mu\nu}$, as well as the vierbein as a perturbation, $v_{A\mu}=\eta_{0A\mu}+\kappa c_{A\mu}$, where $\kappa=M_{\rm Pl}^{-1}$. As is shown in [61], the vierbein is not fundamentally necessary for the purposes of perturbation theory and can be completely eliminated in favor of the metric. Introducing the vierbein introduces six local Lorentz gauge-degrees-of-freedom which can be eliminated by imposing the "Lorentz symmetric gauge,"

$$0 = v_{A\alpha}\eta^{\alpha\beta}\eta_{B\beta}-v_{B\alpha}\eta^{\alpha\beta}\eta_{A\beta}. \tag{B5}$$

Inserting $v_{A\alpha}=\eta_{0A\alpha}+\kappa c_{A\alpha}$ we have

$$0 = c_{A\alpha}\eta^{\alpha\beta}\eta_{B\beta}-c_{B\alpha}\eta^{\alpha\beta}\eta_{A\beta} \tag{B6}$$

$$= c_{AB}-c_{BA}. \tag{B7}$$

This implies that $c_{A\alpha}$ is symmetric. From the definition of the vierbein one can derive

$$c_{\mu\nu}=\frac{1}{2}h_{\mu\nu}+\mathcal{O}(\kappa). \tag{B8}$$

The procedure is then to insert this gauge-fixed vierbein into the above action and expand everything to leading order in κ. The main expressions are

$$\sqrt{-g} = 1 + \frac{\kappa h}{2} + \cdots,$$
$$\omega_{\mu AB} = \frac{\kappa}{2}(\partial_B h_{A\mu} - \partial_A h_{B\mu}) + \cdots,$$
$$\Gamma^{\rho}_{\mu\nu} = \frac{\kappa}{2}\eta^{\rho\lambda}(h_{\mu\lambda,\nu} + h_{\nu\lambda,\mu} - h_{\mu\nu,\lambda}) + \cdots, \quad \text{(B9)}$$

$$\begin{aligned} i\sqrt{-g}\bar{\psi}\gamma^A v_A^\mu \nabla_\mu \psi \supset\ & i\frac{h\kappa}{2}\bar{\psi}\gamma^\mu\partial_\mu\psi + i\bar{\psi}\gamma^\lambda\frac{\kappa}{2}\eta^{\mu\sigma}h_{\lambda\sigma}\partial_\mu\psi \\ & - i\kappa\bar{\psi}\gamma^\alpha\eta_{\alpha\phi}h^{\phi\mu}\partial_\mu\psi \\ & + \frac{\kappa}{8}i\bar{\psi}\gamma^\mu\partial_\alpha h_{\beta\mu}[\gamma^\alpha,\gamma^\beta]\psi, \\ e\sqrt{-g}\bar{\psi}\gamma^A v_A^\mu A_\mu\psi \supset\ & e\frac{\kappa}{2}h\bar{\psi}\gamma^\mu A_\mu\psi + e\frac{\kappa}{2}\bar{\psi}\gamma^\lambda\eta^{\mu\sigma}h_{\lambda\sigma}A_\mu\psi \\ & - e\kappa\bar{\psi}\gamma^\alpha\eta_{\alpha\lambda}A_\mu\psi h^{\mu\lambda}, \\ & - m\sqrt{-g}\bar{\psi}\psi \supset -m\frac{\kappa}{2}h\bar{\psi}\psi. \end{aligned} \quad \text{(B10)}$$

The first operator $ih\kappa\bar{\psi}\gamma^\mu\partial_\mu\psi/2$ gives rise to a term in the Feynman rule (with all ingoing momenta and p_1 being aligned with the direction of charge flow and p_2 being misaligned with the direction of charge flow),

$$i\frac{h\kappa}{2}\bar{\psi}\gamma^\mu\partial_\mu\psi \to \frac{i\kappa}{2}\eta^{\mu\nu}\gamma^\lambda p_{2\lambda} = \frac{i\kappa}{2}\eta^{\mu\nu}\not{p}_2, \quad \text{(B11)}$$

$$i\bar{\psi}\gamma^\lambda\frac{\kappa}{2}\eta^{\mu\sigma}h_{\lambda\sigma}\partial_\mu\psi \to \frac{i\kappa}{2}\gamma^{(\mu}p_2^{\nu)}, \quad \text{(B12)}$$

$$-i\kappa\bar{\psi}\gamma^\alpha\eta_{\alpha\phi}h^{\phi\mu}\partial_\mu\psi \to -i\kappa\gamma^{(\mu}p_2^{\nu)}, \quad \text{(B13)}$$

$$\frac{\kappa}{8}i\bar{\psi}\gamma^\mu\partial_\alpha h_{\beta\mu}[\gamma^\alpha,\gamma^\beta]\psi \to -\frac{i\kappa}{8}p_{3\alpha}\gamma^{(\mu}[\gamma^{\nu)},\gamma^\alpha], \quad \text{(B14)}$$

$$-m\frac{\kappa}{2}h\bar{\psi}\psi \to -im\frac{\kappa}{2}\eta^{\mu\nu}. \quad \text{(B15)}$$

Summing up gives the graviton-fermion-fermion vertex,

$$V^{\mu\nu}_{h\psi\bar{\psi}} = \frac{i}{2M_{\rm Pl}}\left(\eta^{\mu\nu}\not{p}_2 - \gamma^{(\mu}p_2^{\nu)} - \frac{1}{4}p_{3\alpha}\gamma^{(\mu}[\gamma^{\nu)},\gamma^\alpha] - m\eta^{\mu\nu}\right), \quad \text{(B16)}$$

at which point we can use the identity

$$\gamma^{(\mu}[\gamma^{\nu)},\gamma^\alpha] = \gamma^\mu\eta^{\alpha\nu} + \gamma^\nu\eta^{\alpha\mu} - 2\eta^{\mu\nu}\gamma^\alpha \quad \text{(B17)}$$

to give

$$V^{\mu\nu}_{h\psi\bar{\psi}} = \frac{i}{4M_{\rm Pl}}(\gamma^{(\mu}(p_1-p_2)^{\nu)} - \eta^{\mu\nu}(\not{p}_1 - \not{p}_2 + 2m)). \quad \text{(B18)}$$

The other graviton-matter interaction vertex is

$$V^{\mu\nu;\alpha}_{h\psi\bar{\psi}A} = \frac{ie}{2M_{\rm Pl}}(\eta^{\mu\nu}\gamma^\alpha - \gamma^{(\mu}\eta^{\nu)\alpha}). \quad \text{(B19)}$$

2. Photon wave function renormalization

The graviton exchange diagrams are the same as in the scalar QED case; however, the wave function renormalization factor is different due to the spinor-electron loop. As there is no photon-photon-fermion-fermion vertex, the four-point photon amplitude at one-loop involves only a subset of diagrams that we needed in the scalar QED case. The 1PI self-energy from the one diagram Fig. 5(b) gives (in $\overline{\rm MS}$)

$$\begin{aligned} \Pi^{\mu\nu} &= -\frac{ie^2}{2\pi^2}(\eta^{\mu\nu}k^2 - k^\mu k^\nu)\int_0^1 {\rm d}x x(1-x)\ln\left(\frac{\mu^2}{m^2 + x(1-x)k^2}\right) = (\eta^{\mu\nu}k^2 - k^\mu k^\nu)\Pi(k^2), \\ \Rightarrow \Pi(0) &= -\frac{ie^2}{12\pi^2}\ln\frac{\mu^2}{m^2}. \end{aligned} \quad \text{(B20)}$$

As in the scalar QED case we have

$$Z_A = \frac{1}{1 + i\Pi(0)} \Rightarrow Z_A = 1 - \frac{e^2}{12\pi^2}\ln\frac{\mu^2}{m^2} + \mathcal{O}(e^4). \quad \text{(B21)}$$

Then, the one-loop corrected amplitude from the tree diagrams would be

$$\begin{aligned} \mathcal{A}^{\rm I}_{\rm tree} &= \frac{1}{M_{\rm Pl}^2}\frac{s^4}{stu}\left(1 - \frac{e^2}{6\pi^2}\ln\frac{\mu^2}{m^2} + \cdots\right) = \frac{1}{M_{\rm Pl}^2}\left(-\frac{s^2}{t} - \frac{s^2}{u}\right)\left(1 - \frac{e^2}{6\pi^2}\ln\frac{\mu^2}{m^2} + \cdots\right), \\ \mathcal{A}^{\rm II}_{\rm tree} &= \frac{1}{M_{\rm Pl}^2}\frac{u^4}{stu}\left(1 - \frac{e^2}{6\pi^2}\ln\frac{\mu^2}{m^2} + \cdots\right) = \frac{1}{M_{\rm Pl}^2}\left(-\frac{u^2}{t} - \frac{u^2}{s}\right)\left(1 - \frac{e^2}{6\pi^2}\ln\frac{\mu^2}{m^2} + \cdots\right). \end{aligned} \quad \text{(B22)}$$

3. Nongravitational contributions

The only one-loop nongravitational diagrams we have are the box diagrams. The box amplitude is

$$\begin{aligned} i\mathcal{A}_{\text{box}} = (-1)(ie)^4 \int \frac{\mathrm{d}^d p}{(2\pi)^d} [&\mathrm{Tr}(\not{\epsilon}_1 S_F^{13} \not{\epsilon}_3 S_F^{34} \not{\epsilon}_4 S_F^{42} \not{\epsilon}_2 S_F^{21}) + \mathrm{Tr}(\not{\epsilon}_1 S_F^{12} \not{\epsilon}_2 S_F^{24} \not{\epsilon}_4 S_F^{43} \not{\epsilon}_3 S_F^{31}) \\ &+ \mathrm{Tr}(\not{\epsilon}_1 S_F^{14} \not{\epsilon}_4 S_F^{42} \not{\epsilon}_2 S_F^{23} \not{\epsilon}_3 S_F^{31}) + \mathrm{Tr}(\not{\epsilon}_1 S_F^{13} \not{\epsilon}_3 S_F^{32} \not{\epsilon}_2 S_F^{24} \not{\epsilon}_4 S_F^{41}) \\ &+ \mathrm{Tr}(\not{\epsilon}_1 S_F^{14} \not{\epsilon}_4 S_F^{43} \not{\epsilon}_3 S_F^{32} \not{\epsilon}_2 S_F^{21}) + \mathrm{Tr}(\not{\epsilon}_1 S_F^{12} \not{\epsilon}_2 S_F^{23} \not{\epsilon}_3 S_F^{34} \not{\epsilon}_4 S_F^{41})], \end{aligned} \tag{B23}$$

where S_F^{ij} is the Dirac fermion Feynman propagator connecting vertices with ingoing photons of momenta k_i and k_j. The factor of (-1) is related to the one fermion loop. We have used the *Mathematica* package "Package-X" to compute the forward limit box amplitude for helicity configurations I and II [62]. The amplitude for configuration III is zero in the forward limit, and the other two configurations are given by

$$\begin{aligned} \mathcal{A}^{\text{I}}_{\text{box}}(s, t=0) = \left(\frac{-e^4}{4\pi^2 s^2}\right) \Bigg\{ &-4(s-m^2)\sqrt{s(s+4m^2)}\log\left(\frac{\sqrt{s(s+4m^2)}+2m^2+s}{2m^2}\right) \\ &- 2(s-2m^2)\sqrt{s(s-4m^2)}\log\left(\frac{\sqrt{s(s-4m^2)}+2m^2-s}{2m^2}\right) \\ &+ (-4m^4-2m^2 s+s^2)\log^2\left(\frac{\sqrt{s(s+4m^2)}+2m^2+s}{2m^2}\right) \\ &+ 2m^2(s-2m^2)\log^2\left(\frac{\sqrt{s(s-4m^2)}+2m^2-s}{2m^2}\right) + 6s^2 \Bigg\} \end{aligned} \tag{B24}$$

and

$$\begin{aligned} \mathcal{A}^{\text{II}}_{\text{box}}(s, t=0) = \left(\frac{e^4}{4\pi^2 s^2}\right) \Bigg\{ &-4(s+m^2)\sqrt{s(s-4m^2)}\log\left(\frac{\sqrt{s(s-4m^2)}+2m^2-s}{2m^2}\right) \\ &- 2(s+2m^2)\sqrt{s(s+4m^2)}\log\left(\frac{\sqrt{s(s+4m^2)}+2m^2+s}{2m^2}\right) \\ &+ (4m^4-2m^2 s-s^2)\log^2\left(\frac{\sqrt{s(s-4m^2)}+2m^2-s}{2m^2}\right) \\ &+ 2m^2(s+2m^2)\log^2\left(\frac{\sqrt{s(s+4m^2)}+2m^2+s}{2m^2}\right) - 6s^2 \Bigg\}. \end{aligned} \tag{B25}$$

So as to compare with [40], we may work below the electron mass, and expanding this in powers of s/m^2 finally gives the same contribution for configurations I and II to that order,

$$\mathcal{A}^{\text{I}}_{\text{box}}(s, t=0) = \frac{11e^4 s^2}{720\pi^2 m^4} + \mathcal{O}(s^3/m^6) \quad \text{and} \quad \mathcal{A}^{\text{II}}_{\text{box}}(s, t=0) = \frac{11e^4 s^2}{720\pi^2 m^4} + \mathcal{O}(s^3/m^6). \tag{B26}$$

4. One-loop graviton exchange

The diagrams relevant for the one-loop graviton exchange are similar to those provided in the scalar QED case (see Appendix A 5). Referring back to Fig. 6, there is no analog to types $\mathfrak{b}$ and $\mathfrak{d}$ diagrams for spinor QED. In practice all type $\mathfrak{c}$ diagrams vanish for spinor QED so in what follows we can simply focus our discussion on type $\mathfrak{a}$ diagrams, and we only provide our results for configurations I and II.

Configurations I and II of the amplitude from type $\mathfrak{a}$ diagrams are given by (expanded in the forward limit)

$$M_{\text{Pl}}^2 \mathcal{A}^{\text{I}}_{\mathfrak{a}}(s, t=0) = -\frac{e^2 s^2}{6\pi^2 t}\ln\frac{\mu^2}{m^2} - \frac{11e^2 s^2}{360\pi^2 m^2} + \frac{e^2 s}{6\pi^2}\ln\frac{\mu^2}{m^2} + \frac{e^2 s}{12\pi^2} \tag{B27}$$

and

$$M_{\rm Pl}^2\mathcal{A}_{\rm a}^{\rm II}(s,t=0)=-\frac{e^2s^2}{6\pi^2t}\ln\frac{\mu^2}{m^2}-\frac{11e^2s^2}{360\pi^2m^2}-\frac{e^2s}{6\pi^2}\ln\frac{\mu^2}{m^2}-\frac{e^2s}{12\pi^2}. \tag{B28}$$

For both configurations, the first term is exactly what cancels against the one-loop wave function renormalization of the tree diagrams (i.e., the t-pole cancellation), while the third term cancels the remaining μ dependence from the wave function renormalization leading to a final amplitude that is μ independent as it should be. These results are consistent with [40]. The full expressions are

$$\begin{aligned}M_{\rm Pl}^2\mathcal{A}_{\rm a}^{\rm I}(s,t=0)=&-\frac{e^2s^2}{6\pi^2t}\ln\frac{\mu^2}{m^2}+\frac{e^2}{720\pi^2m^2s}\left\{120m^2s^2\ln\frac{\mu^2}{m^2}+s(-1560m^4+410m^2s-11s^2)\right.\\&-120m^2(s-5m^2)\sqrt{s(4m^2+s)}\ln\left(\frac{\sqrt{s(4m^2+s)}+2m^2+s}{2m^2}\right)\\&\left.+180m^4(2m^2-s)\ln^2\left(\frac{\sqrt{s(4m^2+s)}+2m^2+s}{2m^2}\right)\right\}\end{aligned} \tag{B29}$$

and

$$\begin{aligned}M_{\rm Pl}^2\mathcal{A}_{\rm a}^{\rm II}(s,t=0)=&-\frac{e^2s^2}{6\pi^2t}\ln\frac{\mu^2}{m^2}-\frac{e^2}{720\pi^2m^2s}\left\{120m^2s^2\ln\frac{\mu^2}{m^2}+s(1560m^4+410m^2s+11s^2)\right.\\&+120m^2(5m^2+s)\sqrt{s(s-4m^2)}\ln\left(\frac{\sqrt{s(s-4m^2)}+2m^2-s}{2m^2}\right)\\&\left.+180m^4(2m^2+s)\ln^2\left(\frac{\sqrt{s(s-4m^2)}+2m^2-s}{2m^2}\right)\right\}.\end{aligned} \tag{B30}$$

[1] T. N. Pham and T. N. Truong, Evaluation of the derivative quartic terms of the meson chiral Lagrangian from forward dispersion relation, Phys. Rev. D **31**, 3027 (1985).

[2] B. Ananthanarayan, D. Toublan, and G. Wanders, Consistency of the chiral pion pion scattering amplitudes with axiomatic constraints, Phys. Rev. D **51**, 1093 (1995).

[3] A. Adams, N. Arkani-Hamed, S. Dubovsky, A. Nicolis, and R. Rattazzi, Causality, analyticity and an IR obstruction to UV completion, J. High Energy Phys. 10 (2006) 014.

[4] B. Bellazzini, Softness and amplitudes' positivity for spinning particles, J. High Energy Phys. 02 (2017) 034.

[5] C. de Rham, S. Melville, A. J. Tolley, and S.-Y. Zhou, UV complete me: Positivity bounds for particles with spin, J. High Energy Phys. 03 (2018) 011.

[6] C. de Rham, S. Melville, A. J. Tolley, and S.-Y. Zhou, Positivity bounds for scalar field theories, Phys. Rev. D **96**, 081702 (2017).

[7] C. Cheung and G. N. Remmen, Positive signs in massive gravity, J. High Energy Phys. 04 (2016) 002.

[8] J. Bonifacio, K. Hinterbichler, and R. A. Rosen, Positivity constraints for pseudolinear massive spin-2 and vector Galileons, Phys. Rev. D **94**, 104001 (2016).

[9] C. de Rham, S. Melville, A. J. Tolley, and S.-Y. Zhou, Massive Galileon positivity bounds, J. High Energy Phys. 09 (2017) 072.

[10] C. de Rham, S. Melville, and A. J. Tolley, Improved positivity bounds and massive gravity, J. High Energy Phys. 04 (2018) 083.

[11] C. de Rham, S. Melville, A. J. Tolley, and S.-Y. Zhou, Positivity bounds for massive spin-1 and spin-2 fields, J. High Energy Phys. 03 (2019) 182.

[12] L. Alberte, C. de Rham, A. Momeni, J. Rumbutis, and A. J. Tolley, Positivity constraints on interacting spin-2 fields, J. High Energy Phys. 03 (2020) 097.

[13] L. Alberte, C. de Rham, A. Momeni, J. Rumbutis, and A. J. Tolley, Positivity constraints on interacting pseudo-linear spin-2 fields, J. High Energy Phys. 07 (2020) 121.

[14] Z.-Y. Wang, C. Zhang, and S.-Y. Zhou, Generalized elastic positivity bounds on interacting massive spin-2 theories, J. High Energy Phys. 04 (2021) 217.

[15] C. Zhang and S.-Y. Zhou, Positivity bounds on vector boson scattering at the LHC, Phys. Rev. D **100**, 095003 (2019).
[16] Q. Bi, C. Zhang, and S.-Y. Zhou, Positivity constraints on aQGC: Carving out the physical parameter space, J. High Energy Phys. 06 (2019) 137.
[17] G. N. Remmen and N. L. Rodd, Consistency of the standard model effective field theory, J. High Energy Phys. 12 (2019) 032.
[18] C. Zhang and S.-Y. Zhou, Convex Geometry Perspective to the (Standard Model) Effective Field Theory Space, Phys. Rev. Lett. **125**, 201601 (2020).
[19] G. N. Remmen and N. L. Rodd, Signs, spin, SMEFT: Positivity at dimension six, arXiv:2010.04723.
[20] G. N. Remmen and N. L. Rodd, Flavor Constraints from Unitarity and Analyticity, Phys. Rev. Lett. **125**, 081601 (2020).
[21] K. Yamashita, C. Zhang, and S.-Y. Zhou, Elastic positivity vs extremal positivity bounds in SMEFT: A case study in transversal electroweak gauge-boson scatterings, J. High Energy Phys. 01 (2021) 095.
[22] T. Trott, Causality, unitarity and symmetry in effective field theory, arXiv:2011.10058.
[23] Q. Bonnefoy, E. Gendy, and C. Grojean, Positivity bounds on minimal flavor violation, J. High Energy Phys. 04 (2021) 115.
[24] B. Fuks, Y. Liu, C. Zhang, and S.-Y. Zhou, Positivity in electron-positron scattering: Testing the axiomatic quantum field theory principles and probing the existence of UV states, Chin. Phys. C **45**, 023108 (2021).
[25] M. B. Green and C. Wen, Superstring amplitudes, unitarily, and Hankel determinants of multiple zeta values, J. High Energy Phys. 11 (2019) 079.
[26] Y.-t. Huang, J.-Y. Liu, L. Rodina, and Y. Wang, Carving out the space of open-string S-matrix, J. High Energy Phys. 04 (2021) 195.
[27] A. J. Tolley, Z.-Y. Wang, and S.-Y. Zhou, New positivity bounds from full crossing symmetry, arXiv:2011.02400.
[28] B. Bellazzini, J. Elias Miró, R. Rattazzi, M. Riembau, and F. Riva, Positive moments for scattering amplitudes, arXiv:2011.00037.
[29] S. Caron-Huot and V. Van Duong, Extremal effective field theories, arXiv:2011.02957.
[30] A. Sinha and A. Zahed, Crossing Symmetric Dispersion Relations in QFTs, Phys. Rev. Lett. **126**, 181601 (2021).
[31] N. Arkani-Hamed, Y. Huang, and T.-C. Huang, The EFThedron, J. High Energy Phys. 05 (2021) 259.
[32] A. Guerrieri, J. Penedones, and P. Vieira, S-matrix bootstrap for effective field theories: Massless pions, arXiv:2011.02802.
[33] I. Drummond and S. Hathrell, QED Vacuum Polarization in a background gravitational field and its effect on the velocity of photons, Phys. Rev. D **22**, 343 (1980).
[34] T. J. Hollowood and G. M. Shore, Causality violation, gravitational shockwaves and UV completion, J. High Energy Phys. 03 (2016) 129.
[35] C. de Rham and A. J. Tolley, Speed of gravity, Phys. Rev. D **101**, 063518 (2020).
[36] C. de Rham and A. J. Tolley, Causality in curved spacetimes: The speed of light and gravity, Phys. Rev. D **102**, 084048 (2020).
[37] L. Alberte, C. de Rham, S. Jaitly, and A. J. Tolley, Positivity bounds and the massless spin-2 pole, Phys. Rev. D **102**, 125023 (2020).
[38] C. Vafa, The string landscape and the Swampland, arXiv:hep-th/0509212.
[39] H. Ooguri and C. Vafa, On the geometry of the string landscape and the Swampland, Nucl. Phys. **B766**, 21 (2007).
[40] C. Cheung and G. N. Remmen, Infrared consistency and the weak gravity conjecture, J. High Energy Phys. 12 (2014) 087.
[41] Y. Hamada, T. Noumi, and G. Shiu, Weak Gravity Conjecture from Unitarity and Causality, Phys. Rev. Lett. **123**, 051601 (2019).
[42] B. Bellazzini, M. Lewandowski, and J. Serra, Positivity of Amplitudes, Weak Gravity Conjecture, and Modified Gravity, Phys. Rev. Lett. **123**, 251103 (2019).
[43] W.-M. Chen, Y.-T. Huang, T. Noumi, and C. Wen, Unitarity bounds on charged/neutral state mass ratios, Phys. Rev. D **100**, 025016 (2019).
[44] C. Cheung, J. Liu, and G. N. Remmen, Proof of the weak gravity conjecture from black hole entropy, J. High Energy Phys. 10 (2018) 004.
[45] G. J. Loges, T. Noumi, and G. Shiu, Thermodynamics of 4D dilatonic black holes and the weak gravity conjecture, Phys. Rev. D **102**, 046010 (2020).
[46] C. Cheung, J. Liu, and G. N. Remmen, Entropy bounds on effective field theory from rotating dyonic black holes, Phys. Rev. D **100**, 046003 (2019).
[47] G. Goon and R. Penco, Universal Relation Between Corrections to Entropy and Extremality, Phys. Rev. Lett. **124**, 101103 (2020).
[48] S. Andriolo, D. Junghans, T. Noumi, and G. Shiu, A tower weak gravity conjecture from infrared consistency, Fortschr. Phys. **66**, 1800020 (2018).
[49] L. Aalsma, A. Cole, and G. Shiu, Weak gravity conjecture, black hole entropy, and modular invariance, J. High Energy Phys. 08 (2019) 022.
[50] S. Cremonini, C. R. Jones, J. T. Liu, and B. McPeak, Higher-derivative corrections to entropy and the weak gravity conjecture in anti-de sitter space, J. High Energy Phys. 09 (2020) 003.
[51] L. Aalsma, A. Cole, G. J. Loges, and G. Shiu, A new spin on the weak gravity conjecture, J. High Energy Phys. 03 (2021) 085.
[52] J. Tokuda, K. Aoki, and S. Hirano, Gravitational positivity bounds, J. High Energy Phys. 11 (2020) 054.
[53] M. Herrero-Valea, R. Santos-Garcia, and A. Tokareva, Massless positivity in graviton exchange, arXiv:2011.11652.
[54] N. Arkani-Hamed, L. Motl, A. Nicolis, and C. Vafa, The string landscape, black holes and gravity as the weakest force, J. High Energy Phys. 06 (2007) 060.
[55] T. J. Hollowood and G. M. Shore, The causal structure of QED in curved spacetime: Analyticity and the refractive index, J. High Energy Phys. 12 (2008) 091.
[56] G. Shore, A local effective action for photon gravity interactions, Nucl. Phys. **B646**, 281 (2002).

[57] B. Heidenreich, M. Reece, and T. Rudelius, Evidence for a sublattice weak gravity conjecture, J. High Energy Phys. 08 (2017) 025.

[58] B. Heidenreich, M. Reece, and T. Rudelius, The weak gravity conjecture and emergence from an ultraviolet cutoff, Eur. Phys. J. C **78**, 337 (2018).

[59] G. Dvali, Black holes and large N species solution to the hierarchy problem, Fortschr. Phys. **58**, 528 (2010).

[60] G. Dvali and M. Redi, Black hole bound on the number of species and quantum gravity at LHC, Phys. Rev. D **77**, 045027 (2008).

[61] R. Woodard, The Vierbein is irrelevant in perturbation theory, Phys. Lett. **148B**, 440 (1984).

[62] H. H. Patel, Package-X: A Mathematica package for the analytic calculation of one-loop integrals, Comput. Phys. Commun. **197**, 276 (2015).